Electronic Supplementary Material (ESI) for Chemical Science.

A Nine-Ring Fused Terrylene Diimide Exhibits Switching between Red TADF and Near-IR Room Temperature Phosphorescence

Shivangee Jha, Kundan Singh Mehra, Mandira Dey, Sujesh S, Debashree Ghosh,* Pradip Kumar Mondal, Maurizio Polentarutti, and Jeyaraman Sankar*

Department of Chemistry, Indian Institute of Science Education and Research (IISER) Bhopal, Bhopal Bypass Road, Bhopal, India – 462066.

E-mail: sankar@iiserb.ac.in

Table of contents

I. General Information

Materials:

All the chemicals required for synthesis were purchased from Sigma Aldrich, TCI, and Spectrochem and used directly without further purification. All the air or moisture-sensitive reactions were carried out under an argon atmosphere. For all the photophysical studies spectroscopy-grade solvents were used. Compounds synthesized here are purified by silica-gel, alumina column chromatography and size-exclusion column chromatography using Bio-beads from BioRad with tetrahydrofuran (THF) as solvent followed by recrystallization.

Characterization Techniques:

All the NMR experiments were performed either on Bruker Avance 500 or 700 MHz spectrometers in $CDCl_3$ and $C_2D_2Cl_4$ as solvents. Chemical shift values (δ) reported in parts per million (ppm) using residual solvents peak as a reference (^{1}H NMR- 7.26ppm for $CDCl_3$, and ^{1}H NMR- 5.90ppm, for $C_2D_2Cl_4$). Mass spectra for all compounds were acquired on a microTOF-QII high-resolution mass spectrometer using Bruker Daltonics coupled to a Water UPLC system. Matrix-assisted LASER desorption/ionization (MALDI) was recorded using the Bruker Ultra Flextreme MALDI-TOF mass spectrometer.

Photophysical Measurements:

Steady-state absorption spectra were recorded on a Cary 900 UV/VIS/NIR spectrophotometer. Steady-state emission measurements were recorded on a Horiba Scientific Fluoromax 04. Lifetime decay measurements were performed in Delta Flex-01-DD/Horiba time-correlated single-photon counting (TCSPC) using nanosecond pulse deltadiode laser. Phosphorescence emission experiments were performed in phosphorescence division and lifetimes through decay by delay method on Horiba Scientific Fluoromax 04. Low temperature experiments were performed using Liquid Nitrogen Dewar setup. Fluorescence and delayed fluorescence absolute quantum yields were measured using a quanta-phi integrating sphere connected to Fluoromax 04 under ambient conditions. The delayed fluorescence absolute quantum yields were measured with a delay time of 100 μs in phosphorescence devision using a quanta-phi integrating sphere connected to Fluoromax 04.

Formulae:

$$k_f = \phi_f/\tau_f$$

$$k_{df} = \phi_{df}/\tau_{df}$$

$$k_r^s = \phi_f k_f + \phi_{df} k_{df}$$

$$\phi_{ISC} = 1 - \phi_f$$

$$k_{ISC} = k_f(1\text{-}\phi_f)$$

$$k_{RISC} = \frac{k_f k_{df} \phi_{df}}{k_{ISC}\, \phi_f}$$

$$k_{Ph}^r = \phi_{Ph}/\tau_{Ph}$$

Where

k_f = Radiative decay rate constant for fluorescence

k_{df} = Radiative decay rate constant for delayed fluorescence

$k_{r,s}$ = Overall radiative decay rate constant from S_1 to S_0 state including delayed and prompt.

k_{ISC} = Rate constant for intersystem crossing

k_{RISC} = Rate constant for reverse intersystem crossing

$k_{r,Ph}$ = Radiative decay rate constant for phosphorescence

τ_f = Fluorescence lifetime

τ_{df}= Delayed fluorescence lifetime

τ_{Ph} = Phosphorescence lifetime

ϕ_f = Fluorescence quantum yield

ϕ_{df} = Delayed fluorescence quantum yield

ϕ_{Ph} = Phosphorescence quantum yield

ϕ_{ISC} = Efficiency of intersystem crossing

Crystallographic Details:

Single crystal X-ray diffraction (SCXRD) measurements were performed at the X-ray diffraction beamline (XRD1) of the Elettra Synchrotron (Trieste, Italy).[1] The NHV oil (Jena Bioscience, Jena, Germany) was used to dip and mount the crystal on the goniometer head with nylon loops (MiTeGen, Ithaca, USA). The data was collected at 100 K (nitrogen stream supplied through an Oxford Cryostream 700). The data were obtained using a monochromatic wavelength of 0.700 Å by the rotating crystal method on a Pilatus 2M hybrid-pixel area detector (DECTRIS Ltd., Baden-Daettwil, Switzerland). The diffraction data were integrated using XDS.[2] The crystal structure was solved in Olex2[3] using ShelXT[4] solution program by Intrinsic Phasing, and data refinement were done with the ShelXL[5] refinement package through least-squares minimization.

Computational Details:

The ground state geometries of **TDI** and **TDI-cDBT** are optimized at UB3LYP/6-31G(d,p) level of theory. The optimized structures are further used to calculate the low lying excited states at SF-TDDFT/6-31G(d,p) level of theory using Q Chem 5.3 software. All the optimizations are performed in Gaussian 09 software.[6]

II. Synthetic Procedures

Synthesis of Dibenzothiophene-4-boronic acid pinacol ester (DBT-B):

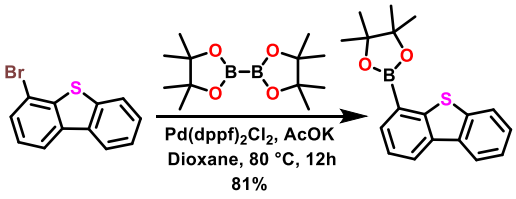

Borylation of 4-Bromodibenzothiophene was done by the modified procedure.[7] In a dry and degassed 100 mL Schlenk flask 4-Bromodibenzothiophene (0.76 mmol, 200 mg), $Pd(dppf)_2Cl_2$ (cat. amount), CH_3COOK (1.75 mmol, 172 mg) and bis(pinacolato)diboron (1.14 mmol, 289 mg) were dissolved in 20 mL dioxane and degassed with argon for 30 minutes. After degassing the mixture was allowed to be stirred at 100 °C for 16 hours. After completion of reaction, the mixture was washed with water 2-3 times and collected over anhydrous Na_2SO_4 using dichloromethane, and concentrated under vacuum. The residue was purified by silica-gel (mess 100-200) chromatography using DCM:Hexane to afford compound **DBT-B** (190.90 mg, 81%) as a white solid. ^{1}H NMR (500 MHz, $CDCl_3$, 298 K) δ (ppm) 8.26 (d, J = 7.8 Hz, 1H), 8.15 (d, 1H), 7.96 (d, J = 7.0 Hz, 1H), 7.88 (d, J= 4.9, 1H), 7.51-7.42 (m, 3H), 1.44 (s, 12H). HRMS (APCI) (m/z): calculated for $C_{18}H_{19}BO_2S$, 310.1308; found, 310.1316.

Synthesis of 1,6-dinitro TDI:

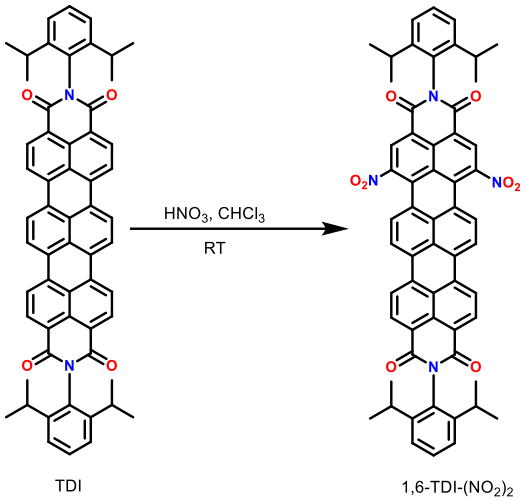

In a dry 100 mL round bottom flask, **TDI** (100 mg, 0.1198 mmol) was dissolved in 50 mL dry $CHCl_3$ and then Nitric acid (531 µL, 11.98 mmol) was added to the solution.[8] The reaction mixture was stirred at room temperature for 1 hour. The excess acid was quenched by a saturated solution of KOH. The reaction mixture was washed with water 2-3 times and then the organic layer was collected over anhydrous Na_2SO_4 using chloroform and concentrated under vacuum. The residue was subjected to neutral alumina column chromatography using DCM/hexane afforded **1,6-TDI-$(NO_2)_2$** as a greenish-blue-coloured product in 30% (33 mg) yield.

^{1}H NMR of **1,6-TDI-$(NO_2)_2$** (500 MHz, $CDCl_3$, 298 K) δ (ppm) 8.95 (s, 2H), 8.82 (d, *J*= 8.0 Hz, 2H), 8.76 (d, *J*= 8.1, 2H), 8.73 (d, *J*= 8.5 Hz, 2H), 8.39 (d, *J*= 8.4 Hz, 2H), 7.56-7.49 (dt, *J*= 12.7, 7.8 Hz, 2H), 7.37 (dd, *J*= 7.5, 5.9 Hz, 4H), 2.77 (dt, *J*= 13.6, 6.8 Hz, 2H), 2.69 (dt, *J*=13.5, 6.7 Hz, 2H), 1.20 (d, *J*=6.7 Hz, 24H). HRMS (APCI) (m/z): calculated for $C_{58}H_{44}N_4O_8$, 925.3232; found, 925.3247.

Synthesis of TDI-sDBT:

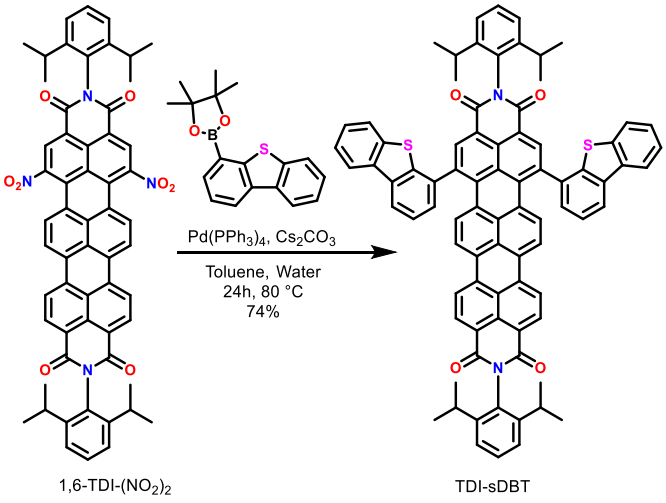

In a dry and degassed schlenk flask **1,6-TDI-$(NO_2)_2$** (0.1 mmol, 100 mg), **DBT-B** (0.2 mmol, 62 mg) and $Pd(PPh_3)_4$ (Cat. amt.) were dissolved in 10 mL dry toluene and degassed with argon for 1 hour. Then an aqueous solution of Cs_2CO_3 (0.4 mmol, 131 mg) in 0.1 mL water was added to the solution and stirred at 90 ºC for 18 hours. After completion of the reaction, the reaction mixture was washed with water and the organic phase was collected over anhydrous Na_2SO_4 using chloroform and concentrated under vacuum. Purification of residue done by silica-gel (mess 100-200) chromatography to afford **TDI-sDBT**

(88 mg, 74%) as blue solid. ^{1}H NMR (500 MHz, $CDCl_3$, 298 K) δ (ppm) 8.87 (s, 1H), 8.83 (s, 1H), 8.83 (s, 2H), 8.32 (d, *J* = 7.7 Hz, 2H), 8.29 (d, *J* = 4.6 Hz, 1H), 8.27 – 8.23 (m, 2H), 8.20 (d, *J* = 7.9 Hz, 1H), 8.20 (d, *J* = 7.9 Hz, 1H), 8.01 – 7.98 (m, 2H), 7.91 (d, *J* = 7.3 Hz, 1H), 7.80 (t, *J* = 7.7 Hz, 1H), 7.69 (d, *J* = 8.7 Hz, 1H), 7.66 (s, 1H), 7.52 – 7.49 (m, 2H), 7.48 – 7.40 (m, 5H), 7.36 (d, *J* = 7.8 Hz, 2H), 7.30 (t, *J* = 8.8 Hz, 4H), 2.85 (dd, *J* = 12.8, 6.6 Hz, 2H), 2.64 (dt, *J* = 13.8, 6.6 Hz, 2H), 1.21 – 1.14 (m, 12H), 1.14 – 1.05 (m, 12H). HRMS (APCI) (m/z): calculated for $C_{58}H_{46}N_2O_4$, 1199.3911; found, 1199.3899.

Synthesis of TDI-cDBT using $FeCl_3$:

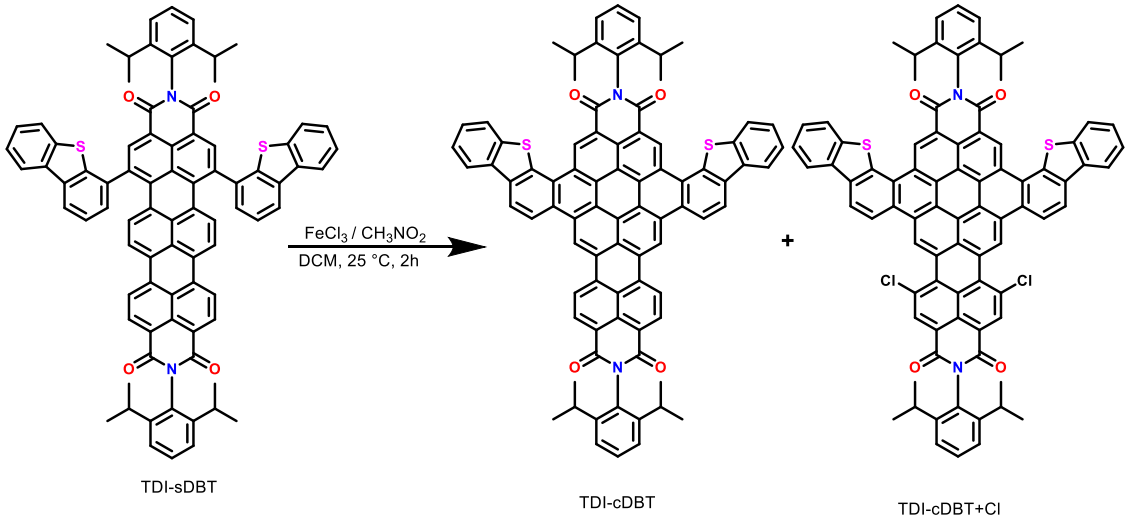

TDI-sDBT TDI-cDBT TDI-cDBT+Cl

In a dry and degassed round bottom flask, **TDI-sDBT** (0.042 mmol, 50 mg) was dissolved in 20 mL methylene chloride. Then a solution of $FeCl_3$ (1.25 mmol, 203 mg) in Nitromethane (8 mL) was added to the solution in a dropwise manner and stirred at room temperature for 2 hours. After completion of the reaction, methanol was added to the solution followed by acid water workup. After workup, the organic layer was collected in chloroform, dried over anhydrous Na_2SO_4, and concentrated under a vacuum. Next, the residue was subjected to silica gel (100-200 mesh) column chromatography. Recrystallization in DCM and methanol give the product **TDI-cDBT** as black-coloured compounds with a yield of 20 mg (40%) with a side product **TDI-cDBT+Cl** in trace amount. ^{1}H NMR for ^{1}H NMR for **TDI-cDBT** (500 MHz, $C_2D_2Cl_4$, 363 K) δ (ppm) 10.57 (s, 2H), 9.75 (s, 2H), 9.30 (s, 2H), 8.99 (s, 2H), 8.54 (d, *J*= 7.9 Hz, 2H), 8.43 (d, *J*= 1.47 Hz, 2H), 7.68 (m, 6H), 7.55 (d, *J*= 7.6 Hz, 2H), 7.50 (m, 4H), 7.34 (d, *J*= 7.8 Hz, 2H), 2.73 (m, 4H), 1.24 (s, 24H). HRMS (APCI) m/z: Calculated for $C_{82}H_{54}N_2O_4S_2$, 1195.3598; found, 1195.3569.

Synthesis of TDI-cDBT using DDQ and CH_3SO_3H:

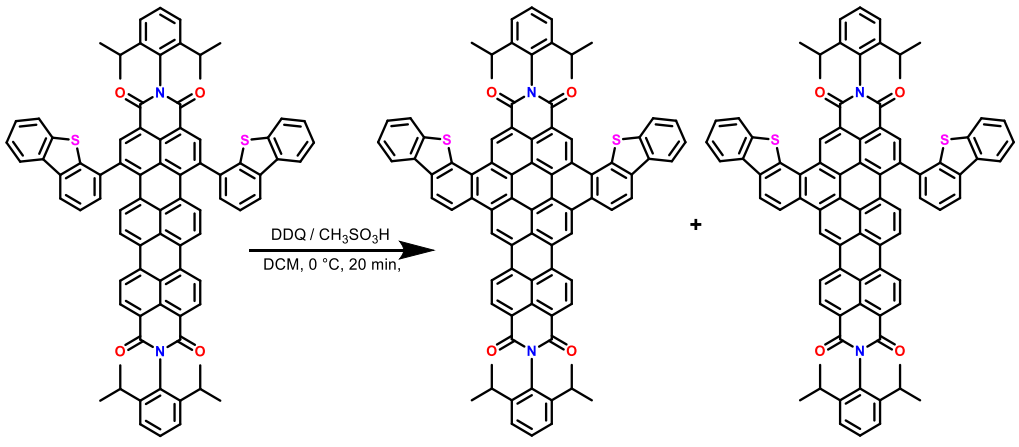

TDI-sDBT TDI-cDBT TDI-scDBT

In a dry and degassed round bottom flask **TDI-sDBT** (0.016 mmol, 20 mg) and DDQ (0.083 mmol, 19 mg) was dissolved in 20 mL methylene chloride. Then 2 mL of methanesulphonic acid was added to the solution in a dropwise manner and stirred at 0 ºC for 20 minutes. After completion of the reaction, a saturated solution of Na_2CO_3 was added to quench the excess of acid. Then the reaction mixture was subjected to water workup and the organic layer was collected in chloroform and dried over anhydrous Na_2SO_4 and concentrated under a vacuum. Next the residue was subjected to silica gel (100-200 mesh) column chromatography. Recrystallization in DCM and methanol give the product **TDI-cDBT** as black coloured compounds with yield of 12 mg (60%) with a side product **TDI-scDBT** (5 mg, 26%).

^{1}H NMR of **TDI-scDBT** (500 MHz, $CDCl_3$, 298 K) δ (ppm) 9.99 (br s, 1H), 9.47 (br s, 1H), 8.82 (d, *J* = 21.4 Hz, 3H), 8.60 (s, 2H), 8.31 (d, *J* = 7.4 Hz, 2H), 8.24 – 8.08 (m, 5H), 7.76 (s, 2H), 7.58 (td, *J* = 8.1, 3.3 Hz, 4H), 7.47 (d, *J* = 7.4 Hz, 3H), 7.43 – 7.36 (m, 5H), 3.08 (br s, *J* = 1.2 Hz, 2H), 2.90 – 2.72 (m, 2H), 1.23 (d, *J* = 22.5 Hz, 24H). MS (MALDI-TOF): Calculated for $C_{82}H_{56}N_2O_4S_2$, 1197.48; found, 1197.58.

III. Photophysical studies

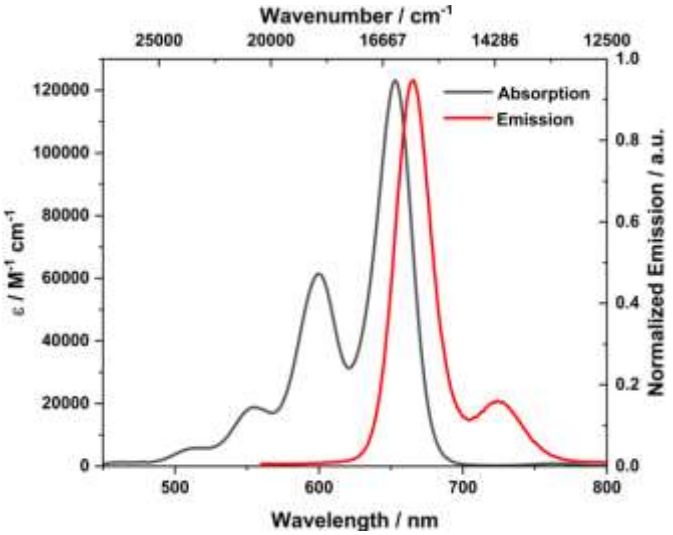

Figure S1. Absorption and Emission spectra of **TDI** in 2x10^{-6} M of toluene (λ_{ex} = 550 nm).

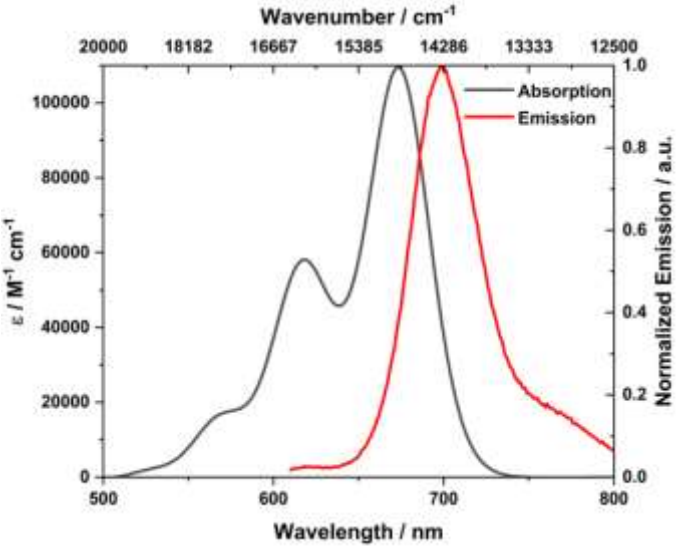

Figure S2. Absorption and Emission spectra of **TDI-sDBT** in 2x10^{-6} M of toluene (λ_{ex} = 550 nm).

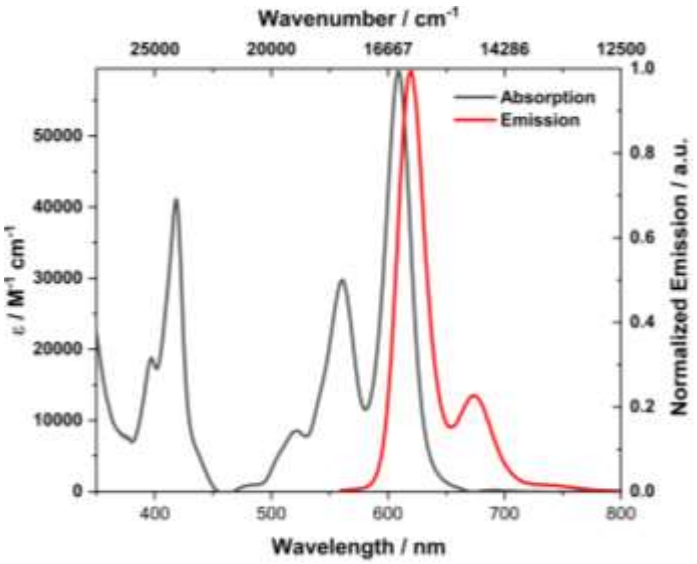

Figure S3. Absorption and Emission spectra of **TDI-cDBT** in $2x10^{-6}$ M of toluene (λ_{ex} = 550 nm).

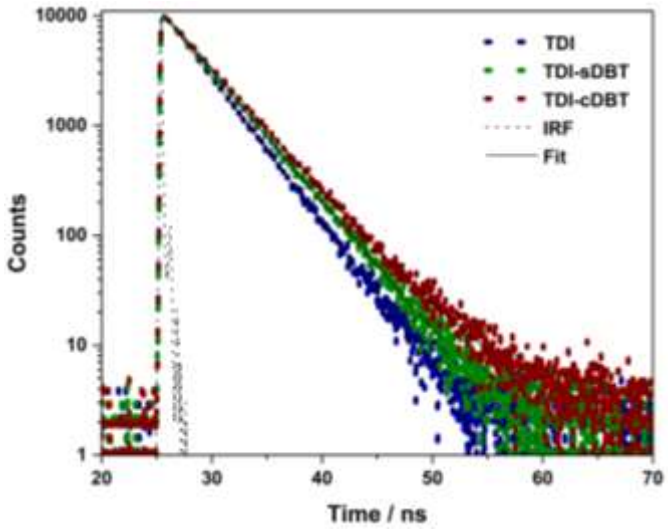

Figure S4. Lifetime decay profile of **TDI** (λ_{ex} = 509 nm, $\lambda_{collected}$ = 666 nm), **TDI-sDBT** (λ_{ex} = 509 nm, $\lambda_{collected}$ = 698 nm) and **TDI-cDBT** (λ_{ex} = 509 nm, $\lambda_{collected}$ = 620 nm) in $2x10^{-6}$ M toluene solution.

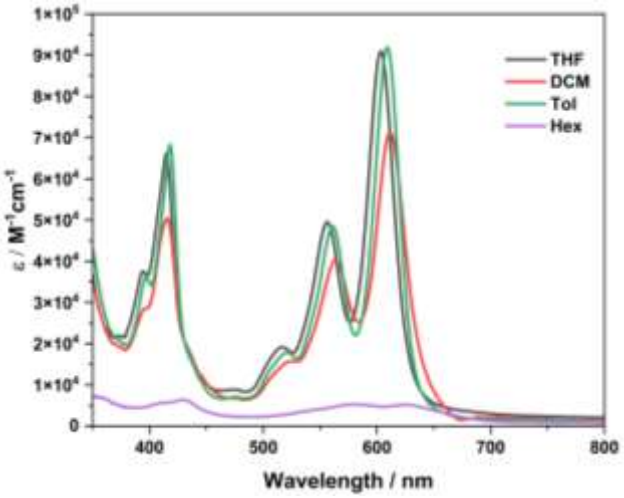

Figure S5. Solvent dependent absorption spectra of **TDI-cDBT** in $2x10^{-6}$ M solution.

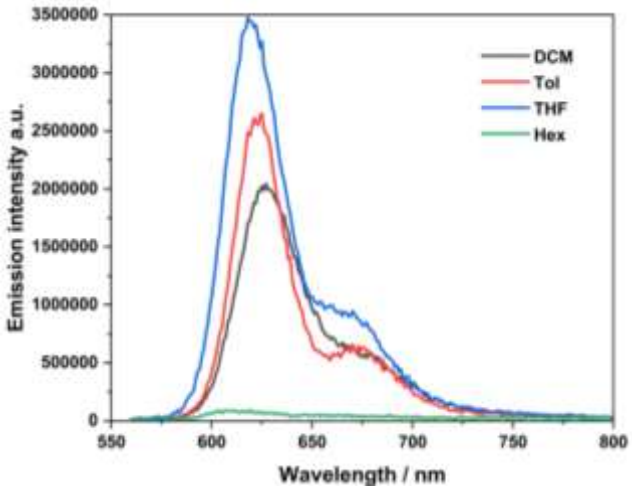

Figure S6. Solvent dependent emission spectra of **TDI-cDBT** in $2x10^{-6}$ M solution (λ_{ex} = 550 nm).

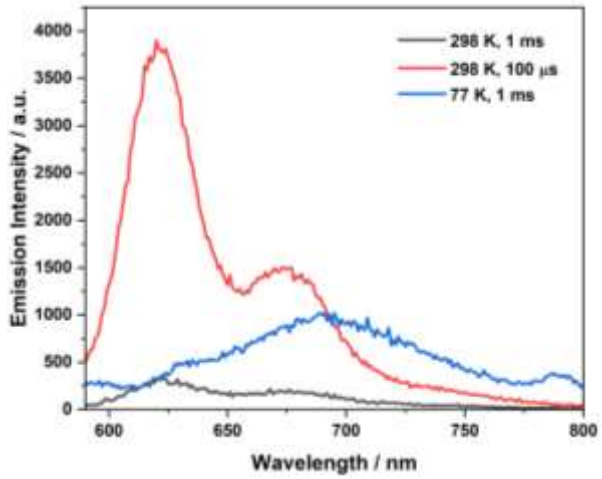

Figure S7. Delayed emission spectra of **TDI-cDBT** in $2x10^{-6}$ M toluene solution (λ_{ex} = 550 nm).

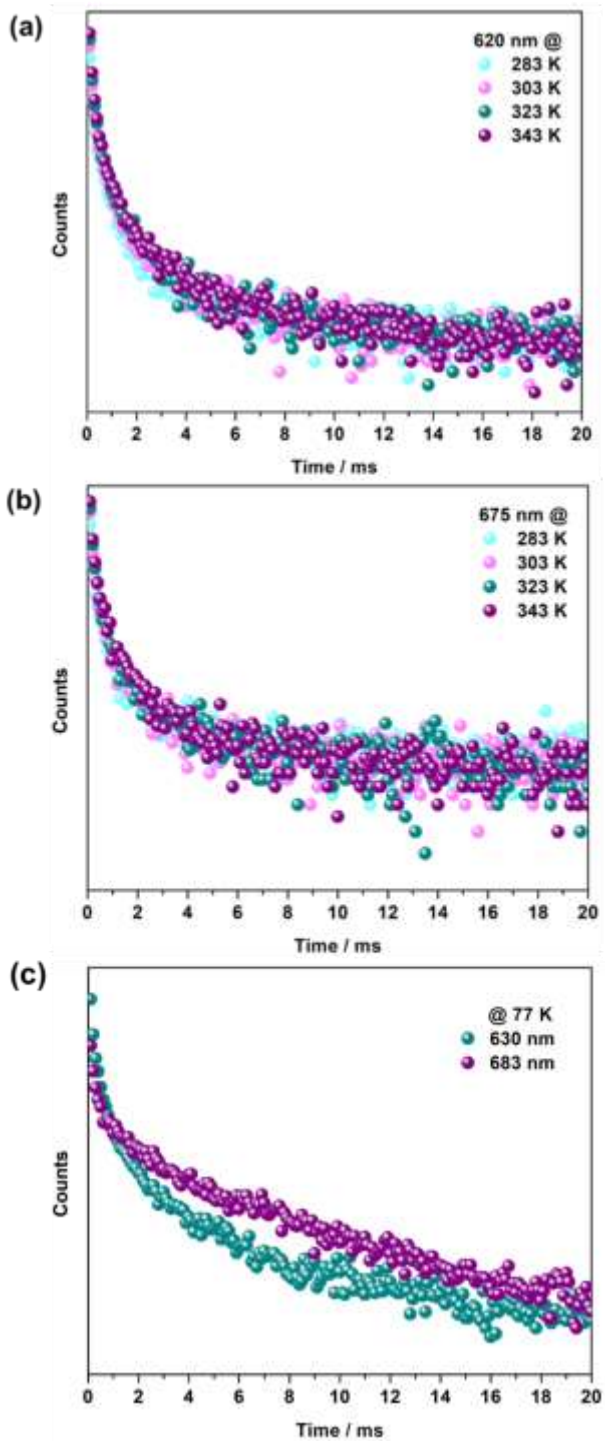

Figure S8. (a and b) Variable temperature; (c) 77 K transient lifetime decay profile of **TDI-cDBT** in $2x10^{-6}$ M toluene solution (λ_{ex} = 550 nm) with initial delay of 100 μs.

Table S1. Variable temperature delayed lifetime of **TDI-cDBT** in $2x10^{-6}$ M toluene solution:

Temperature	τ_{av} [ms] @ 620 nm	τ_{av} [ms] @ 675 nm
77 K	1.3 (630 nm)	2.6 (683 nm)
283 K	1.16	1.11
303 K	0.86	0.96
323 K	0.78	1.10
343 K	0.94	0.85

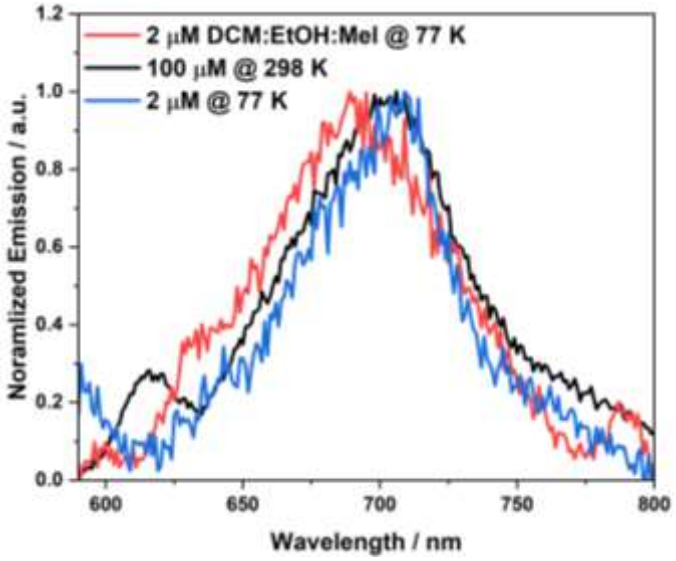

Figure S9. Normalized phosphorescence spectra of **TDI-cDBT** in toluene after 1 ms initial delay for 2μM (blue) and after 100 μs for 100 μM concentration (black) and in DCM:EtOH:MeI (1:1:0.1) solution after an initial delay of 100 μs (red) (λ_{ex} = 550 nm).

Note: The addition of external heavy atom (DCM:EtOH:MeI glass state recorded at 77 K) experiment was conducted to distinguish the phosphorescence band from the delayed emission band.

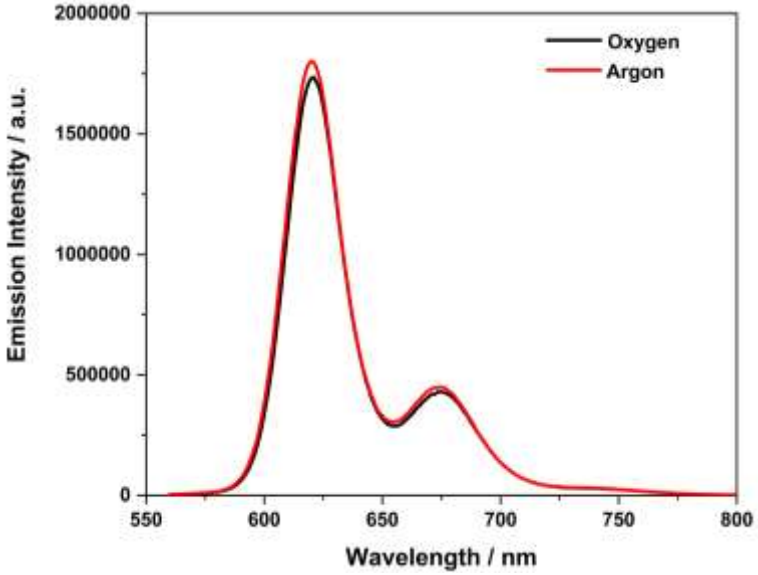

Figure S10: Emission spectra of **TDI-cDBT** under argon and oxygen in $2x10^{-6}$ M toluene solution (λ_{ex} = 550 nm).

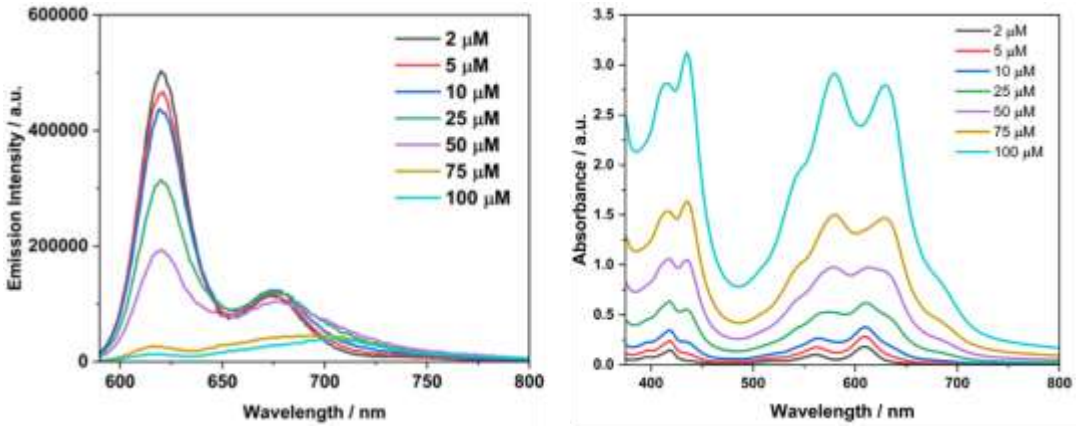

Figure S11. Concentration dependent emission (left) and absorption (right) spectra of **TDI-cDBT** in toluene.

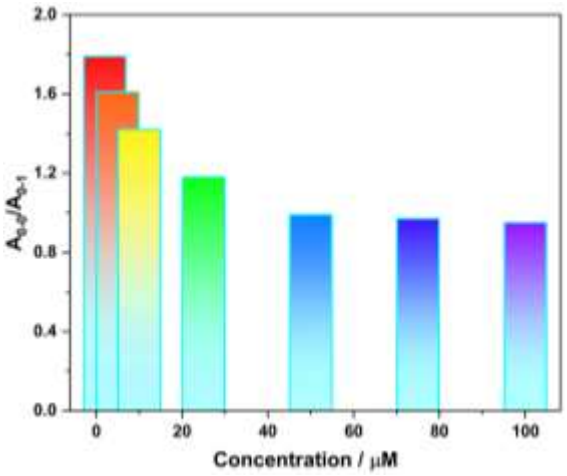

Figure S12. Absorbance ratio $A_{0\text{-}0}$ / $A_{0\text{-}1}$ of **TDI-cDBT** in toluene at variable concentration.

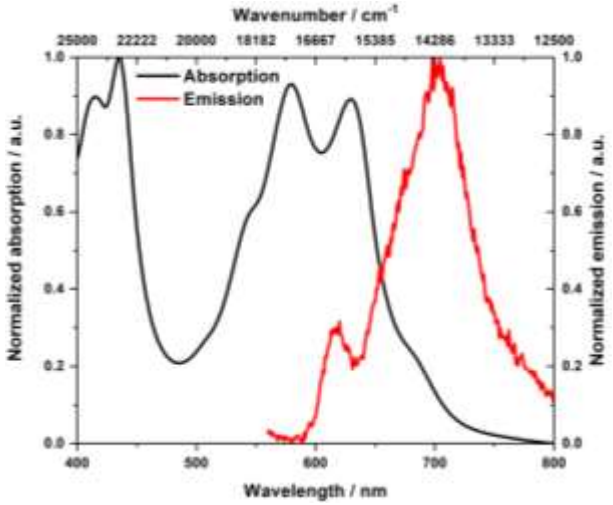

Figure S13. Absorption and Emission spectra of **TDI-cDBT** in $1x10^{-4}$ M of toluene (λ_{ex} = 550 nm).

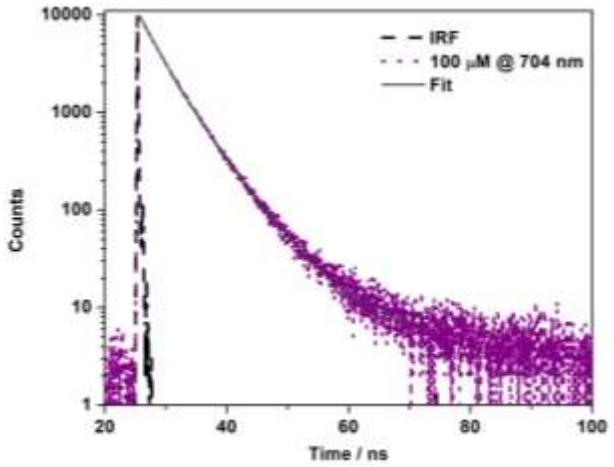

Figure S14. Fluorescence lifetime decay profile of **TDI-cDBT** (λ_{ex} = 509 nm) in 1x10^{-4} M in toluene.

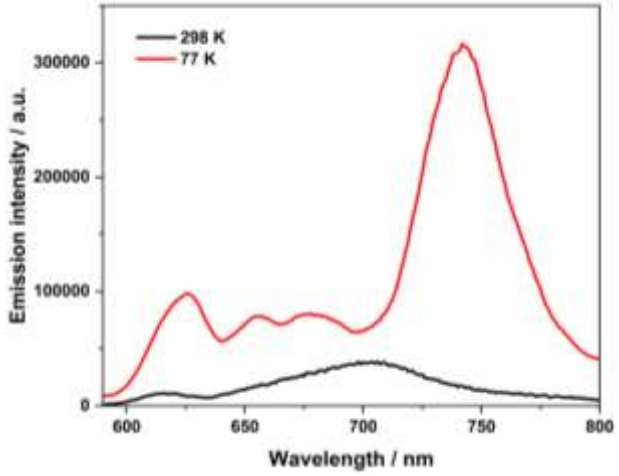

Figure S15. Variable temperature steady state emission spectra of **TDI-cDBT** in 1x10^{-4} M in toluene.

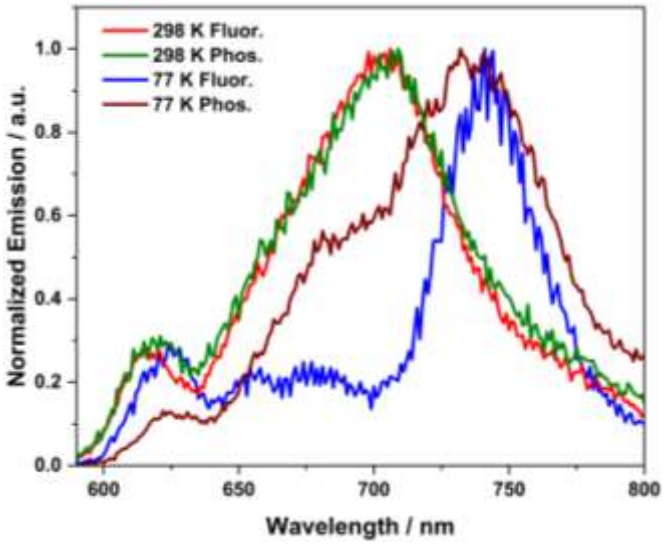

Figure S16. Normalized emission spectra of **TDI-cDBT** in 1x10^{-4} M in toluene.

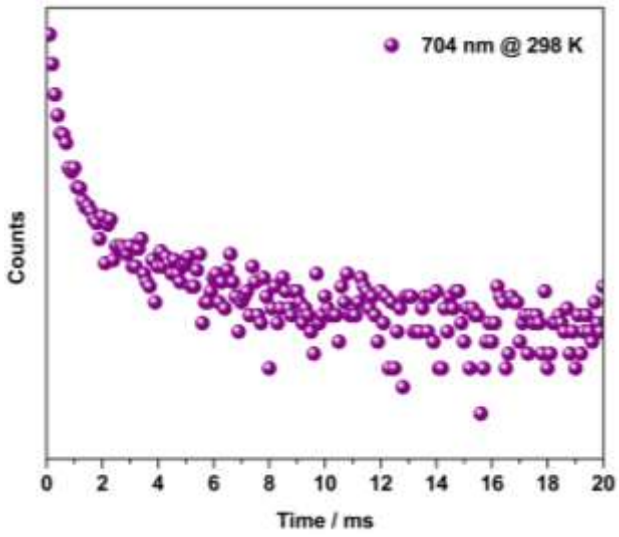

Figure S17. Lifetime decay profile of **TDI-cDBT** (λ_{ex} = 550 nm) in 1x10^{-4} M toluene.

Table S2. Photoluminescence, lifetime and rate constants of **TDI-cDBT**:

Concentration	λ_{fl} [nm]	λ_{phos} [nm]	ϕ_{PL}[a] [%]	ϕ_{fl}[b] [%]	ϕ_{d}[c] [%]	τ_{fl} [ns]	τ_{TADF} [ms]	τ_{phos} [ms]	$\Delta E_{S1\text{-}T1}$[d] [eV]	k_f[e] [s^{-1}]	k_d[f] [s^{-1}]	k_r[g] [s^{-1}]	k_{ISC}[h] [s^{-1}]	k_{RISC}[h] [s^{-1}]
2 μM	620	690	88	41	47	6.0	1.1	6.0[k]	0.05	1.6×10^{8}	9.0×10^{2}	6.5×10^{7}	9.4×10^{7}	1.76×10^{3}
100 μM	704	732	-	15	6[i]	3.9	-	1.8[j]/8.0[k]	0.04	4×10^{7}	33	-	1.5×10^{7}	-

[a] Total photolumniscence quantum yield from S_1-S_0; [b] the prompt fluorescence quantum yield measured using integrating sphere; [c] delayed fluorescence quantum yield measured using integrating sphere after 100 μs delay; [d] Calculated from the onset of fluorescence at 298 K and phosphorescence at 77 K in toluene solution; [e] radiaitve decay rate constant of fluorescence; [f] radiaitve decay rate constant of delayed fluorescence; [g] radiaitve decay rate constant from S_1-S_0; [h] Rate constant for intersystem crossing (k_{ISC}) and reverse intersystem crossing (k_{RISC}) between S_1-T_1; [i] phosphorescence quantum yield measured using integrating sphere after 100 μs delay; triplet transient life time measured at [j] 298 K and [k] 77 K; fl = fluorescence, phos = phosphorescence, TADF= thermally activated delayed fluorescence.

IV. Computational Studies

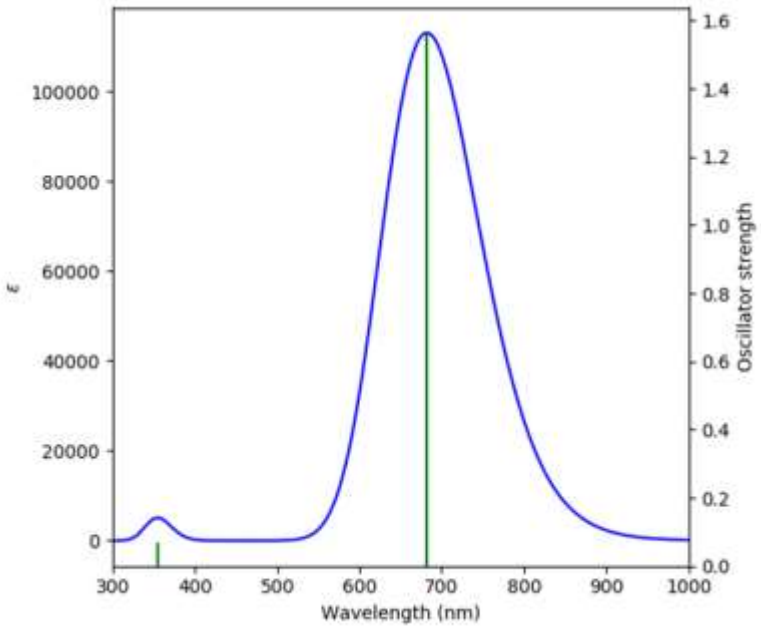

Figure S18. TDDFT predicted absorption spectra of **TDI**.

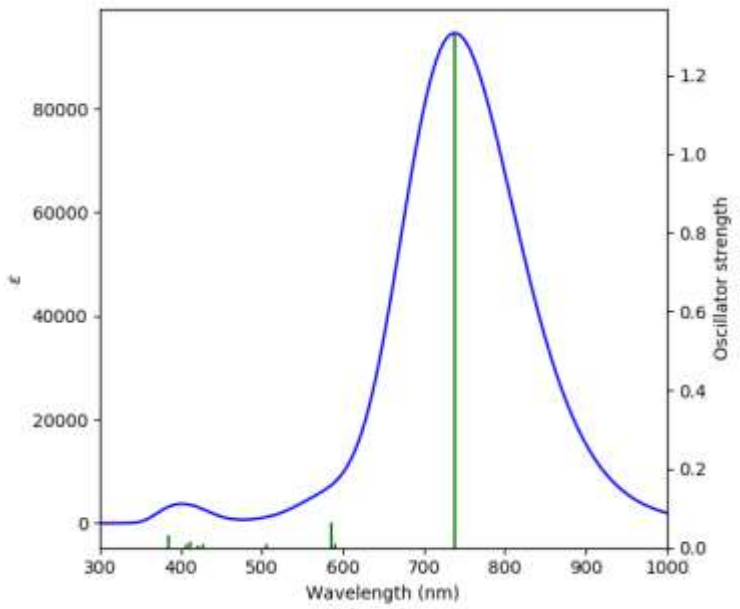

Figure S19. TDDFT predicted absorption spectra of **TDI-sDBT**.

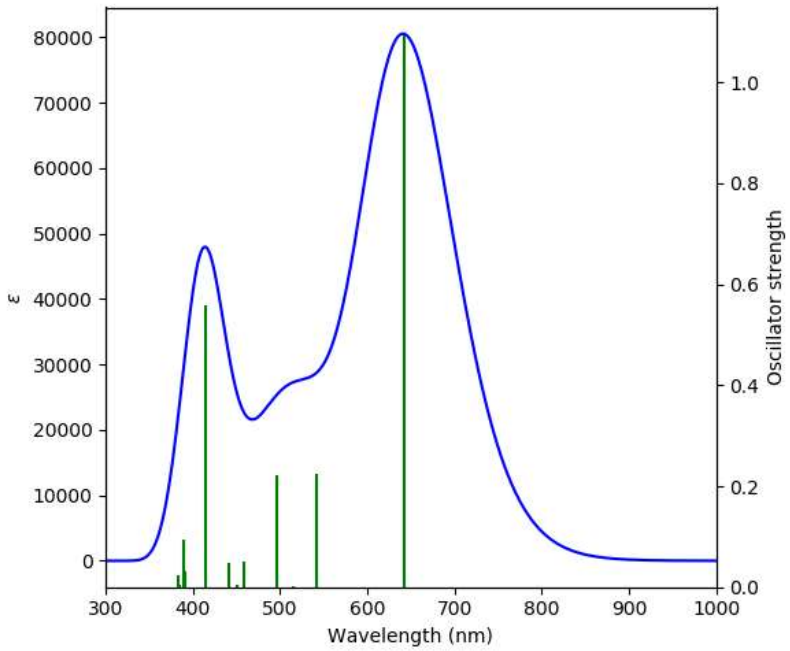

Figure S20. TDDFT predicted absorption spectra of **TDI-cDBT**.

Table S3. Selected TDDFT (B3LYP/6-31G*) calculated wavelength, oscillator strength and major electronic transitions of **TDI**.

Wavelength (nm)	Osc. Strength (f)	Major contributions
681.906242505	1.5603	HOMO->LUMO (101%)
460.873515026	0.0	H-3->LUMO (26%), H-1->LUMO (18%), HOMO->L+1 (56%)
451.130491621	0.0	H-2->LUMO (99%)
450.409390824	0.0	H-1->LUMO (80%)
421.127655352	0.0	H-4->LUMO (96%)
406.50555086	0.0	H-3->LUMO (64%), HOMO->L+1 (34%)
390.046852525	0.0	HOMO->L+2 (93%)
383.199483889	0.0001	H-7->LUMO (83%), HOMO->L+3 (12%)
368.528945136	0.0001	H-9->LUMO (91%)
354.666150845	0.07	H-11->LUMO (87%)
335.219253264	0.0001	H-7->LUMO (11%), HOMO->L+3 (82%)

Table S4. Selected TDDFT (B3LYP/6-31G*) calculated wavelength, oscillator strength and major electronic transitions of **TDI-sDBT**.

Wavelength (nm)	Osc. Strength (f)	Major contributions
738.484680518	1.3036	HOMO->LUMO (100%)
585.853579418	0.0637	H-2->LUMO (99%)
506.471376684	0.0005	H-3->LUMO (99%)
506.326593753	0.0079	H-4->LUMO (99%)
475.217297862	0.0003	H-8->LUMO (14%), H-6->LUMO (24%), HOMO->L+1 (51%)
471.440712621	0.0003	H-6->LUMO (74%), HOMO->L+1 (17%)
439.099706092	0.0001	H-9->LUMO (83%), H-8->LUMO (13%)
426.8546203	0.0103	H-9->LUMO (12%), H-8->LUMO (57%), HOMO->L+1 (24%)
421.14195996	0.0069	H-11->LUMO (14%), H-10->LUMO (76%)
412.044509845	0.0142	HOMO->L+2 (91%)
406.185929145	0.008	H-11->LUMO (82%), H-10->LUMO (12%)
384.268380636	0.0313	H-13->LUMO (72%), H-1->L+1 (11%)

Table S5. Selected TDDFT (B3LYP/6-31G*) calculated wavelength, oscillator strength and major electronic transitions of **TDI-cDBT**.

Wavelength (nm)	Osc. Strength (f)	Major contributions
642.871476782	1.094	HOMO->LUMO (99%)
541.960016664	0.2235	H-1->LUMO (95%)
515.655435918	0.0007	H-2->LUMO (98%)
495.679018959	0.221	H-3->LUMO (98%)
458.657121235	0.0514	H-5->LUMO (12%), H-4->LUMO (83%)
450.376668285	0.0045	H-6->LUMO (93%)
449.935378909	0.0023	H-5->LUMO (82%), H-4->LUMO (13%)
441.20918477	0.0471	HOMO->L+1 (91%)
415.079320429	0.5571	HOMO->L+2 (82%), H-10->LUMO (8%), H-1->LUMO (4%),
390.230999031	0.0308	H-9->LUMO (89%)
389.104296423	0.0931	H-10->LUMO (78%)
384.470953275	0.0036	H-11->LUMO (84%)
382.939101869	0.0233	H-1->L+1 (27%), HOMO->L+3 (69%)

Note: In **TDI-cDBT** the expansion along the molecular shorter axis stabilizes HOMO but destabilizes LUMO and thus causes hypsochromic shift. For **TDI** and **TDI-cDBT** the absorption peak occurs at 774 nm and 688 nm respectively which actually follow the trend observed in the experiments. Previous study on Perylene chromophore[9] also confirms the hypsochromic shift due to expansion in the molecular shorter axis.

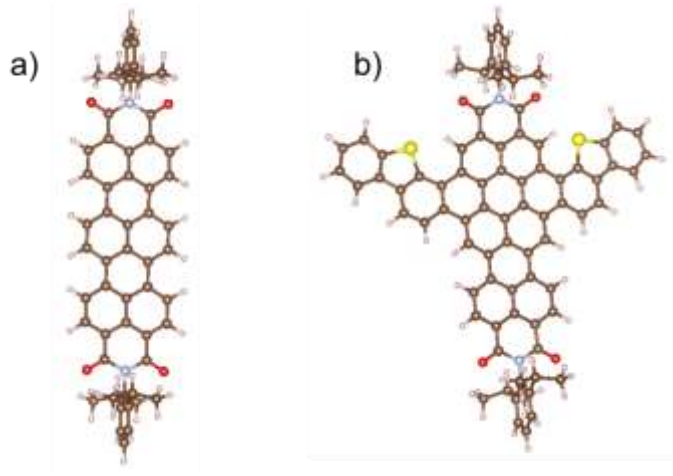

Figure S21: DFT optimized structures of (a) **TDI** and (b) **TDI-cDBT**.

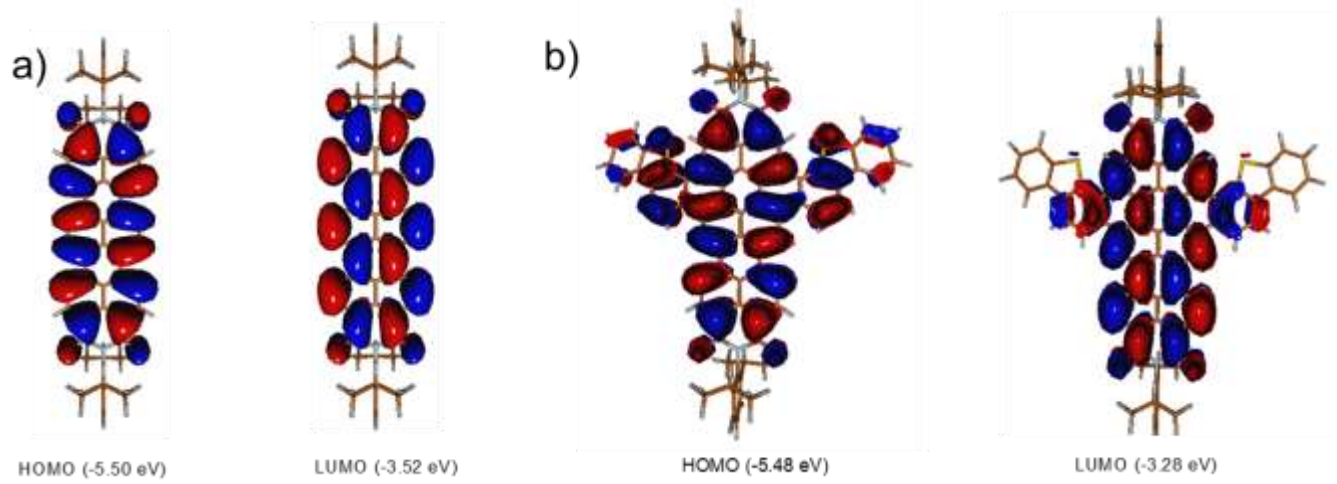

Figure S22: Frontier molecular orbital (FMO) pictures of (a) **TDI** and (b) **TDI-cDBT**.

Table S6. HOMO-LUMO gap and ST gap of **TDI** and **TDI-cDBT** at SF-TDDFT/UB3LYP/6-31G(d,p) level of theory.

System	HOMO-LUMO gap (eV)	ST gap (eV)
TDI	1.98	1.25
TDI-cDBT	2.20	1.54

Note: For linear acenes, increase in conjugation with system size causes the decrease in HOMO-LUMO gap as well as Singlet-Triplet gap (S_0T_1 gap).[10-14] In case of **TDI** conjugation along the molecular long axis reduces the HOMO-LUMO gap[10] as well as ST gap but in **TDI-cDBT** the expansion along the shorter axis breaks the conjugation. As a result, **TDI-cDBT** has a larger ST gap than the **TDI**. The reduction of conjugation of **TDI-cDBT** can be found from the plotting of the average bond length of the rings as shown in figure S23.

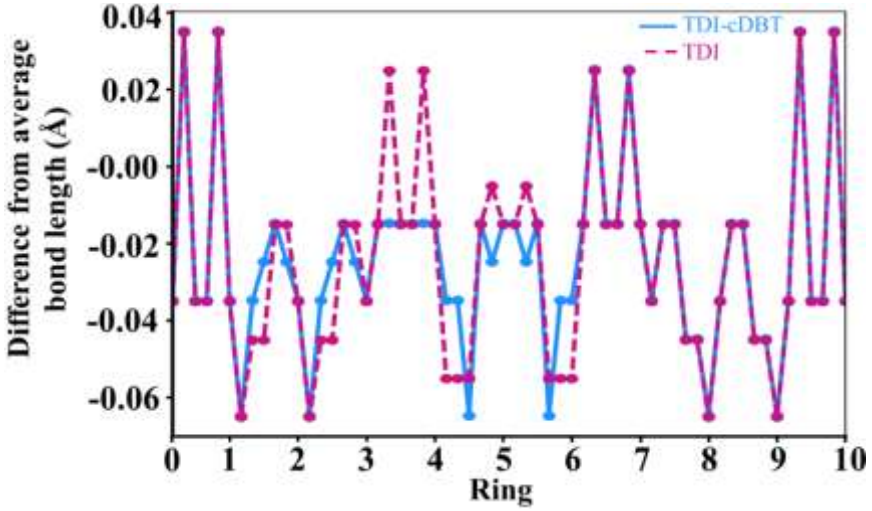

Figure S23: Plot of average bond length of each ring along the molecular large axis of **TDI** and **TDI-cDBT.**

Table S7. Spin-orbit coupling of **TDI** and **TDI-cDBT**.

System	Energy Transition	SOC (cm^{-1})
TDI	S_1-T_1	0.02
	T_1-S_0	0.95
TDI-cBDT	S_1-T_1	0.22
	T_1-S_0	0.58

Note: The S_1 state is the first optically bright state for both the systems and the spin-orbit coupling (SOC) between S_1 and T_1 state is 0.02 cm^{-1} and 0.22 cm^{-1} for **TDI** and **TDI-cDBT** respectively.

Table S8. Low-lying excited states of **TDI** and **TDI-cDBT** at TDDFT/UB3LYP/6-31G(d,p) level of theory.

System	State	Energy (eV)
TDI	T_1	0.86
	S_1	1.95
	T_2	1.98
TDI-cDBT	T_1	1.21
	S_1	2.02
	T_2	2.07
	T_3	2.11

Table S9. Cartesian coordinates of the DFT optimized structures:

TDI:

Symbol	X	Y	Z
O	7.863988	0.18604	2.282613
O	7.863985	-0.18603	-2.28262
N	7.873506	3.20E-05	-3.00E-06
C	0.719379	-1.83E-04	2.00E-05
C	5.030776	-9.70E-05	8.00E-06
C	1.433046	0.102039	1.236557

C	5.741449	-0.09986	-1.22032
C	3.646484	0.198191	2.421139
C	3.601009	-1.43E-04	1.20E-05
C	2.900343	0.101862	1.241745
C	5.043513	-0.19749	-2.41312
H	5.606321	-0.27283	-3.33708
C	3.646483	-0.19848	-2.42111
C	5.741449	0.099706	1.22033
C	2.900341	-0.1022	-1.24171
C	5.043515	0.197283	2.413139
H	5.606323	0.272659	3.337093
C	9.325994	1.20E-04	-8.00E-06
C	7.222796	0.101376	1.244716
C	0.695246	-0.20053	-2.41523
H	1.198423	-0.27979	-3.37077
C	-0.69526	-0.20097	-2.4152
H	-1.19844	-0.28043	-3.37071
C	7.222794	-0.10142	-1.24471
C	1.433043	-0.10245	-1.23651
C	10.00302	-1.22859	0.087292
C	10.00286	1.228917	-0.08731
C	12.09794	2.95E-04	-1.70E-05
H	13.18425	3.63E-04	-2.20E-05
C	9.272112	-2.56285	0.181426
H	8.197069	-2.36136	0.173831
C	11.40213	1.202153	-0.08498
H	11.95246	2.135984	-0.15068
C	11.40228	-1.20165	0.084949
H	11.95273	-2.13541	0.150644
C	9.271789	2.56308	-0.18145
H	8.196771	2.361464	-0.17384
C	9.571174	3.453708	1.039046
H	9.311165	2.938307	1.968155
H	8.993942	4.383401	0.985641
H	10.6315	3.724073	1.087958
C	9.584989	-3.28264	1.506642
H	10.64552	-3.54648	1.579913
H	9.006665	-4.2099	1.584474
H	9.335813	-2.64746	2.361685
C	9.571589	-3.45342	-1.03909
H	9.3115	-2.93803	-1.96819

H	8.994475	-4.38318	-0.98569
H	10.63195	-3.72365	-1.08802
C	9.584559	3.282891	-1.50668
H	10.64506	3.546859	-1.57997
H	9.006123	4.210079	-1.58452
H	9.335446	2.647665	-2.36171
O	-7.86399	-0.19128	-2.28218
O	-7.864	0.191522	2.282158
N	-7.8735	3.40E-05	-4.00E-06
C	-0.71938	-1.74E-04	1.90E-05
C	-5.03078	-5.80E-05	1.00E-05
C	-1.43305	-0.10319	-1.23645
C	-5.74145	0.102411	1.220115
C	-3.64648	-0.20316	-2.42073
C	-3.60102	-1.19E-04	1.40E-05
C	-2.90035	-0.10408	-1.24156
C	-5.04351	0.202524	2.412708
H	-5.60632	0.28016	3.336478
C	-3.64648	0.203017	2.420751
C	-5.74145	-0.10247	-1.2201
C	-2.90035	0.103809	1.24159
C	-5.04351	-0.2026	-2.4127
H	-5.60632	-0.28015	-3.33647
C	-9.32599	8.90E-05	-1.10E-05
C	-7.22279	-0.10431	-1.24448
C	-0.69525	0.200399	2.415256
H	-1.19844	0.279673	3.370783
C	0.695255	0.199968	2.415288
H	1.198435	0.279085	3.370837
C	-7.2228	0.10439	1.244472
C	-1.43305	0.102807	1.236494
C	-10.0029	1.228378	-0.09388
C	-10.003	-1.22816	0.093859
C	-12.0979	1.74E-04	-4.00E-06
H	-13.1842	2.07E-04	1.00E-06
C	-9.27186	2.562007	-0.19561
H	-8.19683	2.360687	-0.18395
C	-11.4022	-1.20127	0.091507
H	-11.9527	-2.13466	0.162388
C	-11.4022	1.201572	-0.09152
H	-11.9525	2.135004	-0.16239

C	-9.27202	-2.56183	0.195596
H	-8.19697	-2.36057	0.183988
C	-9.57438	-3.46118	-1.01773
H	-9.31656	-2.95258	-1.9512
H	-8.99703	-4.39047	-0.95899
H	-10.6348	-3.73193	-1.06224
C	-9.58175	3.272094	-1.52678
H	-10.6422	3.535031	-1.60437
H	-9.00349	4.198933	-1.61002
H	-9.3304	2.630683	-2.3765
C	-9.57422	3.4614	1.017675
H	-9.31647	2.952808	1.951168
H	-8.99682	4.390659	0.958939
H	-10.6346	3.732216	1.062141
C	-9.582	-3.27194	1.526727
H	-10.6425	-3.53481	1.604276
H	-9.00381	-4.19881	1.609966
H	-9.33065	-2.63057	2.376486
H	3.147441	-0.27681	-3.3789
H	3.147442	0.276491	3.378923
H	-3.14743	-0.28354	-3.37833
H	-3.14744	0.283459	3.378359

TDI-sDBT:

Symbol	X	Y	Z
C	-4.4795	2.39911	-0.7607
C	-3.0844	2.44153	-0.5771
C	-2.3137	1.25709	-0.7266
C	-3.0116	-0.001	-0.8197
C	-4.4365	-0.0014	-0.9439
C	-5.1526	1.21548	-0.9846
C	-2.3133	-1.2586	-0.7256
C	-3.0832	-2.4433	-0.574
C	-4.4784	-2.4018	-0.7573
C	-5.1521	-1.2187	-0.9828
C	-0.844	1.24294	-0.7905
C	-0.1321	-0.0005	-0.7796
C	-0.8437	-1.2441	-0.7906
C	-0.0986	2.4113	-0.9742

C	1.29141	2.41112	-1.0061
C	2.02841	1.23552	-0.8866
C	1.30981	-0.0004	-0.8303
C	2.02858	-1.2362	-0.8877
C	1.29174	-2.4118	-1.0079
C	-0.0983	-2.4123	-0.9754
C	3.49555	1.24328	-0.8678
C	4.1992	-0.0002	-0.8659
C	3.49573	-1.2437	-0.8693
C	4.23834	2.42956	-0.835
C	5.63681	2.42342	-0.8244
C	6.3384	1.22643	-0.8337
C	5.62951	-7E-05	-0.8462
C	6.33861	-1.2265	-0.8354
C	5.63721	-2.4236	-0.8277
C	4.23874	-2.4299	-0.8383
C	7.81932	1.2481	-0.8193
N	8.47221	0.00015	-0.8165
C	7.81953	-1.2479	-0.821
C	-6.6219	-1.2449	-1.1732
N	-7.2552	-0.0024	-1.3734
C	-6.6224	1.24072	-1.1751
C	-8.6989	-0.0028	-1.5631
C	9.92689	0.00026	-0.805
C	10.594	-0.0003	0.43367
C	11.9946	-0.0002	0.41711
C	12.7006	0.00048	-0.7835
C	12.0133	0.001	-1.9949
C	10.6131	0.00091	-2.0332
C	-9.5172	-0.0021	-0.417
C	-10.906	-0.0026	-0.6
C	-11.461	-0.0037	-1.8748
C	-10.627	-0.0044	-2.9906
C	-9.2295	-0.004	-2.87
O	-7.2652	-2.2859	-1.1748
O	-7.2662	2.28147	-1.1785
O	8.46347	-2.2899	-0.8138
O	8.46309	2.29016	-0.8108
C	-8.9565	-0.0008	1.00205

C	-9.3618	1.27404	1.76914
C	-9.3615	-1.2744	1.7714
C	-8.4257	-0.0049	-4.1756
C	-7.5863	1.26682	-4.4118
C	-7.5856	-1.2764	-4.4097
C	9.89452	0.00154	-3.3783
C	10.2085	1.27562	-4.1881
C	10.2088	-1.2716	-4.1894
C	9.85467	-0.001	1.76749
C	10.1563	-1.275	2.58198
C	10.1561	1.27227	2.58324
C	-2.5706	-3.786	-0.1531
C	-2.7034	-4.9001	-0.9924
C	-2.0559	-4.0095	1.13756
C	-1.6517	-5.2955	1.56791
C	-1.7738	-6.3828	0.68858
C	-2.3026	-6.1805	-0.5821
S	-1.8517	-2.7863	2.39552
C	-1.2139	-3.9963	3.51199
C	-1.1623	-5.2869	2.93856
C	-0.7941	-3.7618	4.82519
C	-0.3151	-4.8362	5.57216
C	-0.2562	-6.1267	5.01801
C	-0.6765	-6.3546	3.71109
C	-0.8045	3.77102	4.8232
C	-0.3271	4.84708	5.56897
C	-1.2222	4.00297	3.50889
C	-1.1703	5.29247	2.93317
C	-0.6862	6.36184	3.70451
C	-0.2679	6.1365	5.01252
S	-1.8577	2.79059	2.39364
C	-2.0604	4.01144	1.13311
C	-1.6574	5.29837	1.56171
C	-2.5729	3.78533	-0.158
C	-2.7047	4.89776	-0.9997
C	-2.3051	6.17905	-0.5911
C	-1.7785	6.38398	0.68011
H	-5.0559	3.31535	-0.6927
H	-5.0544	-3.3181	-0.6878

H	-0.5972	3.35777	-1.1075
H	1.7902	3.36262	-1.1435
H	1.79064	-3.3632	-1.1462
H	-0.5969	-3.3587	-1.109
H	3.73561	3.38826	-0.8052
H	6.19464	3.35352	-0.8027
H	6.19518	-3.3536	-0.8074
H	3.73619	-3.3888	-0.8098
H	12.5395	-0.0006	1.35651
H	13.787	0.00057	-0.7751
H	12.5727	0.00149	-2.9258
H	-11.559	-0.002	0.26807
H	-12.54	-0.004	-2.0018
H	-11.066	-0.0053	-3.9848
H	-7.8647	-0.0007	0.94205
H	-8.8915	1.28593	2.75911
H	-9.051	2.17262	1.22799
H	-10.446	1.32409	1.91662
H	-8.8912	-1.2844	2.76138
H	-9.0505	-2.1738	1.23185
H	-10.446	-1.3244	1.91899
H	-9.1926	-0.0058	-4.9601
H	-7.2608	1.30019	-5.4581
H	-8.1609	2.17326	-4.2007
H	-6.687	1.29017	-3.7913
H	-7.26	-1.3113	-5.4559
H	-8.1596	-2.1829	-4.1971
H	-6.6861	-1.2982	-3.7893
H	8.81728	0.00132	-3.1875
H	9.62947	1.2867	-5.1187
H	9.9613	2.17557	-3.6168
H	11.2696	1.32666	-4.4567
H	9.96179	-2.1722	-3.6191
H	11.2699	-1.3221	-4.4582
H	9.62975	-1.2818	-5.12
H	8.78052	-0.001	1.56001
H	9.5627	-1.2864	3.50337
H	9.9183	-2.175	2.00676
H	11.2131	-1.3258	2.86729

H	9.56246	1.28257	3.50465
H	9.91787	2.17269	2.00891
H	11.2128	1.32296	2.86859
H	-3.1134	-4.7591	-1.9884
H	-1.4691	-7.3765	1.00274
H	-2.4119	-7.018	-1.2642
H	-0.8399	-2.7659	5.25492
H	0.01523	-4.6723	6.59349
H	0.11942	-6.9518	5.6152
H	-0.6294	-7.3549	3.29063
H	-0.8505	2.77589	5.25471
H	0.00161	4.68516	6.59113
H	-0.6387	7.36143	3.28227
H	0.10647	6.9629	5.6088
H	-3.1131	4.7547	-1.996
H	-2.4135	7.01523	-1.2749
H	-1.4746	7.37841	0.99289

TDI-cDBT:

Symbol	X	Y	Z
C	-3.9073	-2.4201	0.17285
C	-2.5199	-2.4739	-0.0992
C	-1.7983	-1.245	-0.1097
C	-2.494	0.00011	-0.0139
C	-3.8958	0.00001	0.18565
C	-4.5832	-1.2267	0.3127
C	-1.7983	1.24535	-0.1082
C	-2.5199	2.47421	-0.0962
C	-3.9072	2.42018	0.17612
C	-4.5831	1.22661	0.31456
C	-0.3682	-1.2387	-0.1709
C	0.34789	0.00021	-0.1496

C	-0.3682	1.23912	-0.1692
C	0.33737	-2.4646	-0.1953
C	1.74495	-2.4221	-0.1274
C	2.47307	-1.2443	-0.0771
C	1.77106	0.00023	-0.1069
C	2.47289	1.24478	-0.0729
C	1.7448	2.42257	-0.1226
C	0.33731	2.46505	-0.1921
C	3.94312	-1.2482	1.3E-05
C	4.64081	0.0002	0.04173
C	3.94274	1.24865	0.00798
C	4.69002	-2.4284	0.03675
C	6.08557	-2.42	0.11223
C	6.78078	-1.2236	0.15384
C	6.06946	0.00017	0.1196
C	6.78028	1.22389	0.16361
C	6.08458	2.42039	0.13181
C	4.68908	2.42877	0.05542
C	8.26001	-1.2483	0.23393
N	8.90985	0.00012	0.27438
C	8.25949	1.24857	0.24407
C	-6.0365	1.25084	0.61204
N	-6.6724	-0.0003	0.73865
C	-6.0366	-1.2513	0.6098
C	-8.0961	-0.0005	1.0279
C	10.3601	0.00017	0.35288
C	11.1027	0.00345	-0.8406
C	12.4985	0.00342	-0.738
C	13.128	0.00037	0.50275
C	12.3681	-0.0028	1.66825
C	10.9695	-0.003	1.61949
C	-9.0046	0.00734	-0.0446
C	-10.37	0.00725	0.26034
C	-10.813	-0.0008	1.57956
C	-9.8909	-0.0087	2.62187
C	-8.5143	-0.0085	2.36982
O	-6.6665	2.28976	0.74342
O	-6.6668	-2.2904	0.73948
O	8.89973	2.28981	0.28303

O	8.90066	-2.2896	0.26425
C	-8.5546	0.01672	-1.5009
C	-9.0222	-1.2501	-2.2416
C	-9.0084	1.3012	-2.2196
C	-7.5319	-0.0184	3.53521
C	-7.6748	1.24704	4.40148
C	-7.6681	-1.3044	4.37195
C	10.1671	-0.0064	2.91548
C	10.43	-1.2837	3.7352
C	10.428	1.26779	3.74051
C	10.4451	0.00664	-2.2157
C	10.7957	1.28326	-3.0028
C	10.7931	-1.2681	-3.0071
C	-1.8152	3.73107	-0.3225
C	-0.3861	3.72512	-0.3149
C	-2.4573	4.98165	-0.5822
C	-1.725	6.17411	-0.7444
C	-0.3221	6.14177	-0.6604
C	0.32169	4.94518	-0.4683
S	-4.1899	5.28097	-0.8427
C	-3.9133	6.99317	-1.1312
C	-2.5489	7.33032	-1.0389
C	-4.8911	7.94986	-1.4158
C	-4.4865	9.26647	-1.6119
C	-3.1303	9.6225	-1.5244
C	-2.1638	8.66593	-1.2413
C	-4.8908	-7.949	-1.4221
C	-4.4861	-9.2655	-1.6184
C	-3.9131	-6.9924	-1.1369
C	-2.5487	-7.3296	-1.0443
C	-2.1636	-8.6651	-1.247
C	-3.1299	-9.6216	-1.5307
S	-4.1897	-5.2803	-0.8479
C	-2.4572	-4.9811	-0.5867
C	-1.7249	-6.1735	-0.7491
C	-1.8151	-3.7306	-0.3263
C	-0.386	-3.7246	-0.3185
C	0.32175	-4.9447	-0.472

C	-0.322	-6.1412	-0.6646
H	-4.4902	-3.3162	0.32967
H	-4.4901	3.31607	0.33424
H	2.28392	-3.3557	-0.1022
H	2.28369	3.35621	-0.0961
H	4.19481	-3.3909	0.0075
H	6.64799	-3.3469	0.13993
H	6.64658	3.34721	0.16769
H	4.19343	3.39127	0.03457
H	13.0987	0.00582	-1.643
H	14.2128	0.00046	0.5615
H	12.8671	-0.0051	2.63275
H	-11.096	0.01353	-0.5476
H	-11.877	-0.0009	1.79577
H	-10.244	-0.0152	3.64881
H	-7.461	0.01073	-1.5179
H	-10.115	-1.305	-2.2933
H	-8.6409	-1.2556	-3.2686
H	-8.6628	-2.1507	-1.7352
H	-10.101	1.36862	-2.2694
H	-8.6389	2.18863	-1.6977
H	-8.6275	1.32026	-3.2467
H	-6.5184	-0.0107	3.1242
H	-6.9231	1.2521	5.19845
H	-7.5424	2.1487	3.79644
H	-8.6608	1.30016	4.87559
H	-8.6544	-1.3738	4.84326
H	-7.53	-2.1908	3.74603
H	-6.9172	-1.3237	5.1695
H	9.10464	-0.0068	2.65592
H	11.4742	-1.3445	4.06028
H	9.802	-1.2985	4.63282
H	10.2083	-2.1768	3.14377
H	11.4722	1.32894	4.06554
H	10.2047	2.16295	3.15282
H	9.80019	1.2778	4.63833
H	9.36071	0.00758	-2.0726
H	11.8692	1.34389	-3.212

H	10.2694	1.2973	-3.9636
H	10.5108	2.17683	-2.4398
H	11.8665	-1.3303	-3.2161
H	10.5061	-2.1628	-2.447
H	10.2669	-1.2778	-3.968
H	0.25127	7.05517	-0.7826
H	1.40305	4.94793	-0.4619
H	-5.9387	7.67407	-1.4808
H	-5.2294	10.0265	-1.8337
H	-2.8358	10.6558	-1.6793
H	-1.1181	8.95079	-1.1743
H	-5.9384	-7.6732	-1.4873
H	-5.229	-10.025	-1.8407
H	-1.1178	-8.95	-1.1797
H	-2.8354	-10.655	-1.6858
H	1.4031	-4.9475	-0.465
H	0.25138	-7.0546	-0.7868

V. Crystallographic data:

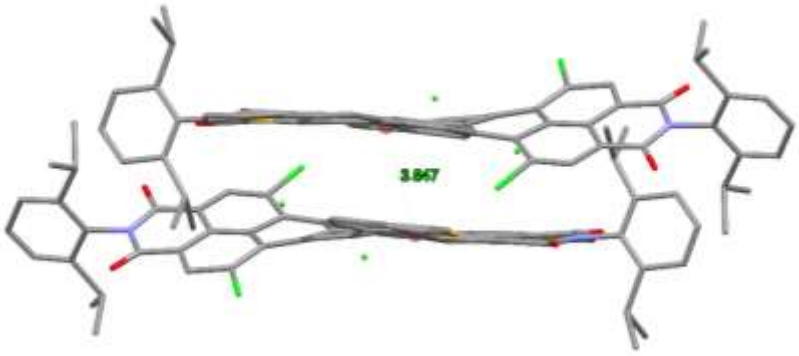

Figure S24. π–π interaction in **TDI-cDBT+Cl** as seen from SCXRD structure.

Table S10. SCXRD data and structure refinement parameters for **TDI-cDBT+Cl**.

Identification code	**TDI-cDBT+Cl**
Empirical formula	$C_{86}H_{56}Cl_{10}N_2O_4S_2$
CCDC number	2293830
Formula weight	1599.94
Temperature/K	100(2)
Wavelength/Å	0.700
Crystal system	Triclinic
Space group	*P* -1
a/Å	16.800(3)
b/Å	18.200(4)
c/Å	18.900(4)
α/°	110.00(3)
β/°	101.00(3)
γ/°	106.00(3)
Volume/Å^3	4953(2)
Z	2
ρ_{calc}g/cm^3	1.073
μ/mm^{-1}	0.345
F(000)	1640
Crystal size/mm^3	0.1 x 0.05 x 0.02
2Θ range for data collection/°	1.19 to 24.5
Index ranges	-19<=h<=19, -20<=k<=21, -22<=l<=22
Reflections collected	43605
Independent reflections	5557
Data/restraints/parameters	16646/862/652
Goodness-of-fit on F^2	1.514
Final R indexes [I>=2σ (I)]	R1 = 0.1993, wR2 = 0.5119
Final R indexes [all data]	R1 = 0.2818, wR2 = 0.5644
Largest diff. peak/hole / e Å^{-3}	0.913 and -0.492

VI. NMR Spectra

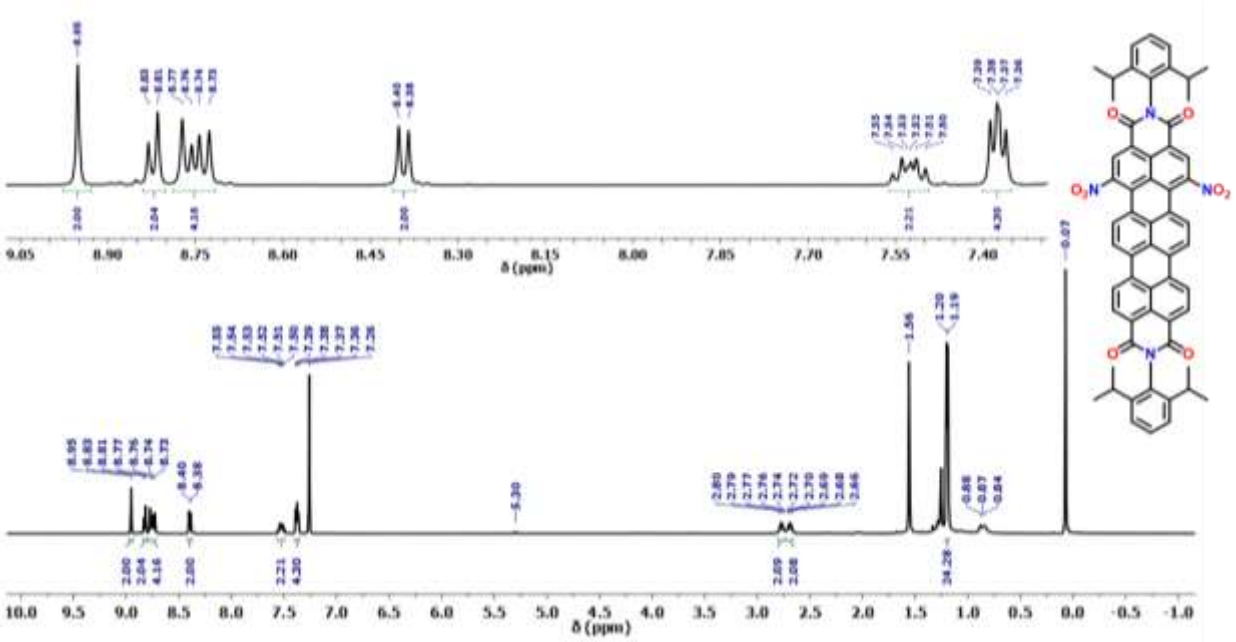

Figure S25. ^{1}H NMR spectra of **1,6-TDI-(NO$_2$)$_2$** (500 MHz, $CDCl_3$, 298 K).

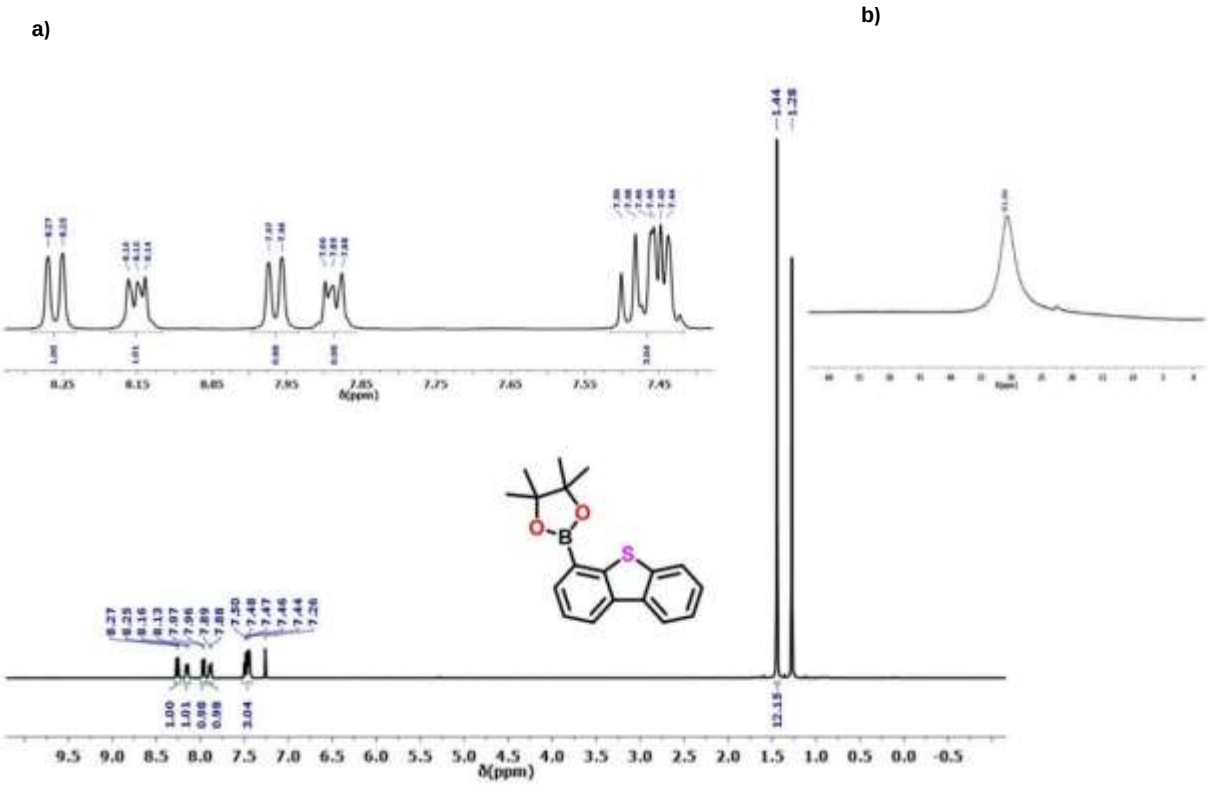

Figure S26. a) ^{1}H and b) ^{11}B-NMR spectra for **DBT-B** (500 MHz, $CDCl_3$, 298 K).

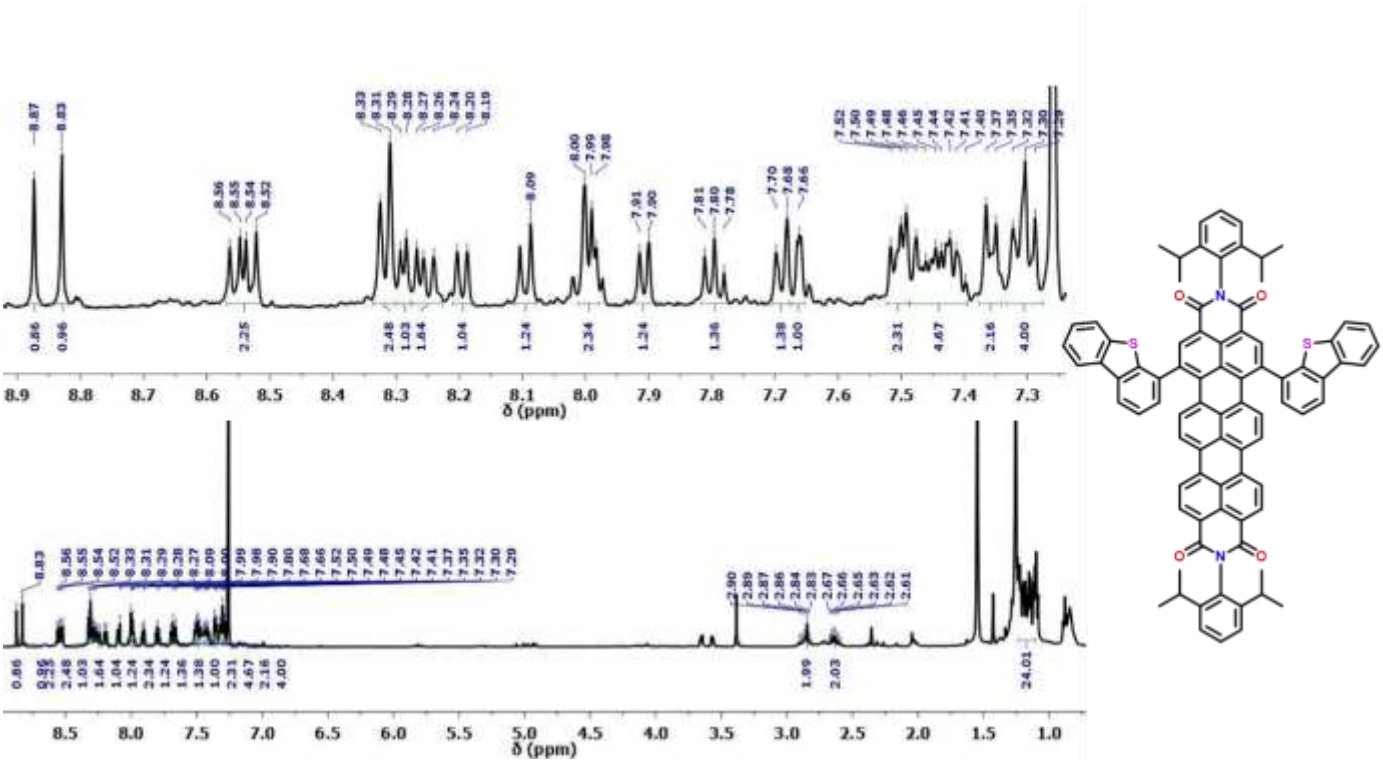

Figure S27. ^{1}H NMR spectra of **TDI-sDBT** (500 MHz, $CDCl_3$, 298 K).

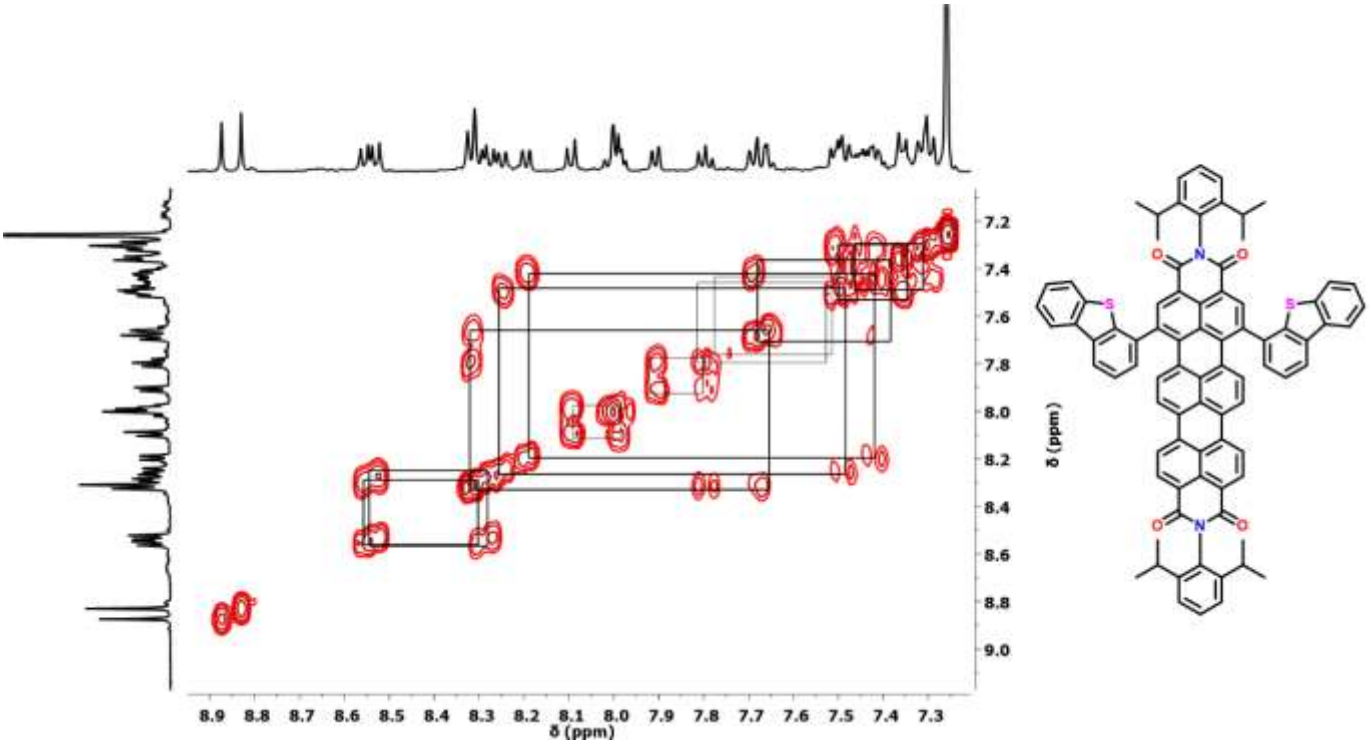

Figure S28. ^{1}H-^{1}H correlation (COSY) NMR spectra of **TDI-sDBT** (500 MHz, $CDCl_3$, 298 K).

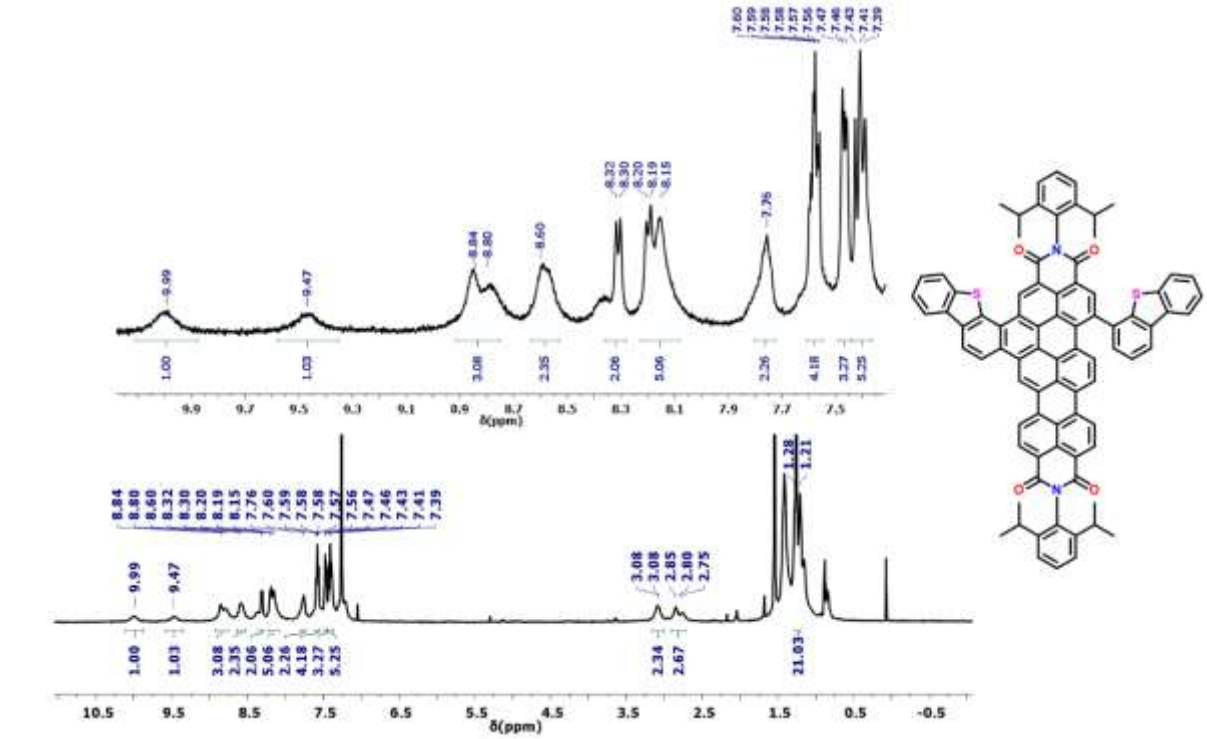

Figure S29. ^{1}H NMR spectra of **TDI-scDBT** (500 MHz, $CDCl_3$, 298 K).

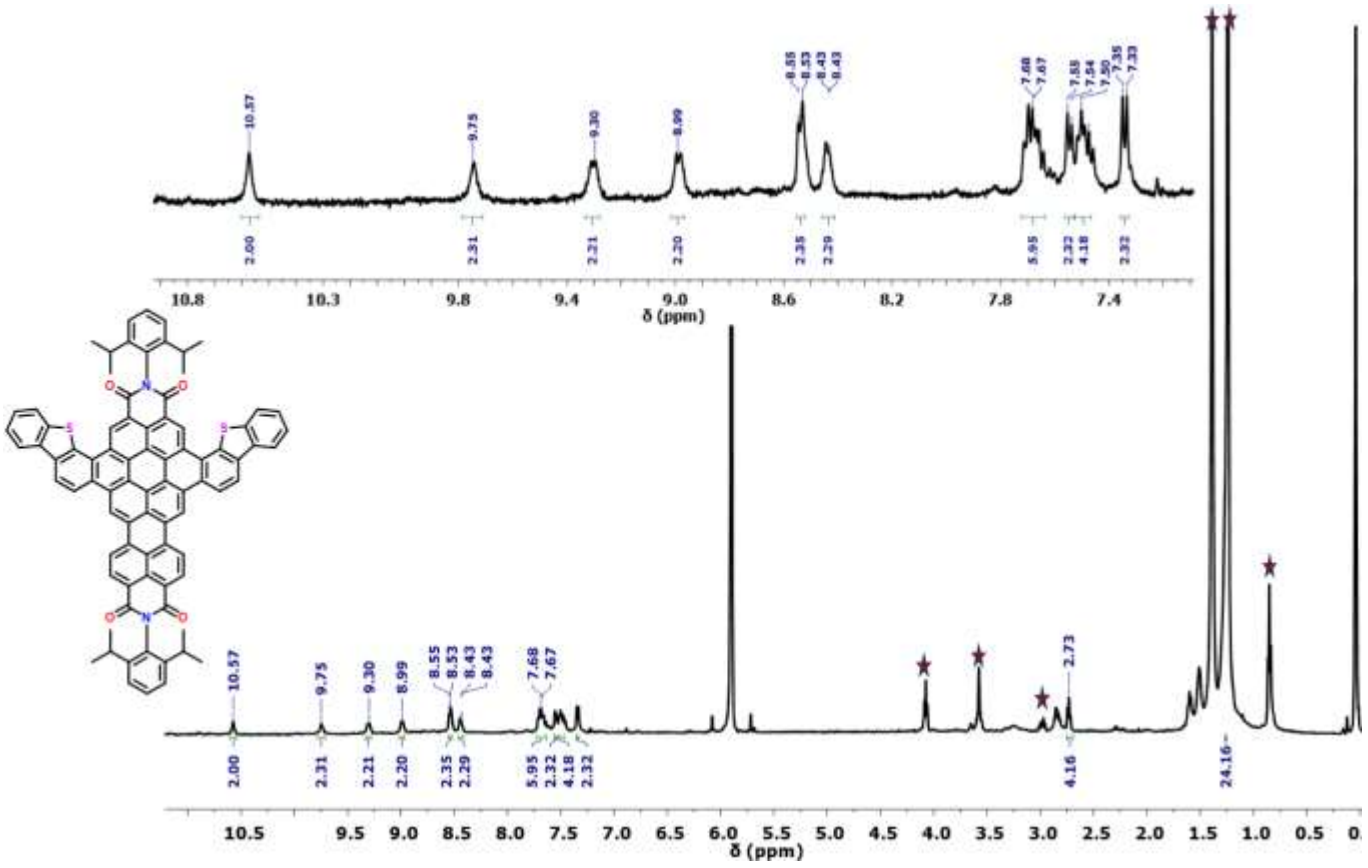

Figure S30. ^{1}H NMR spectra of **TDI-cDBT** (500 MHz, $C_2D_2Cl_4$, 363 K). Asterisk indicates residual solvent peaks.

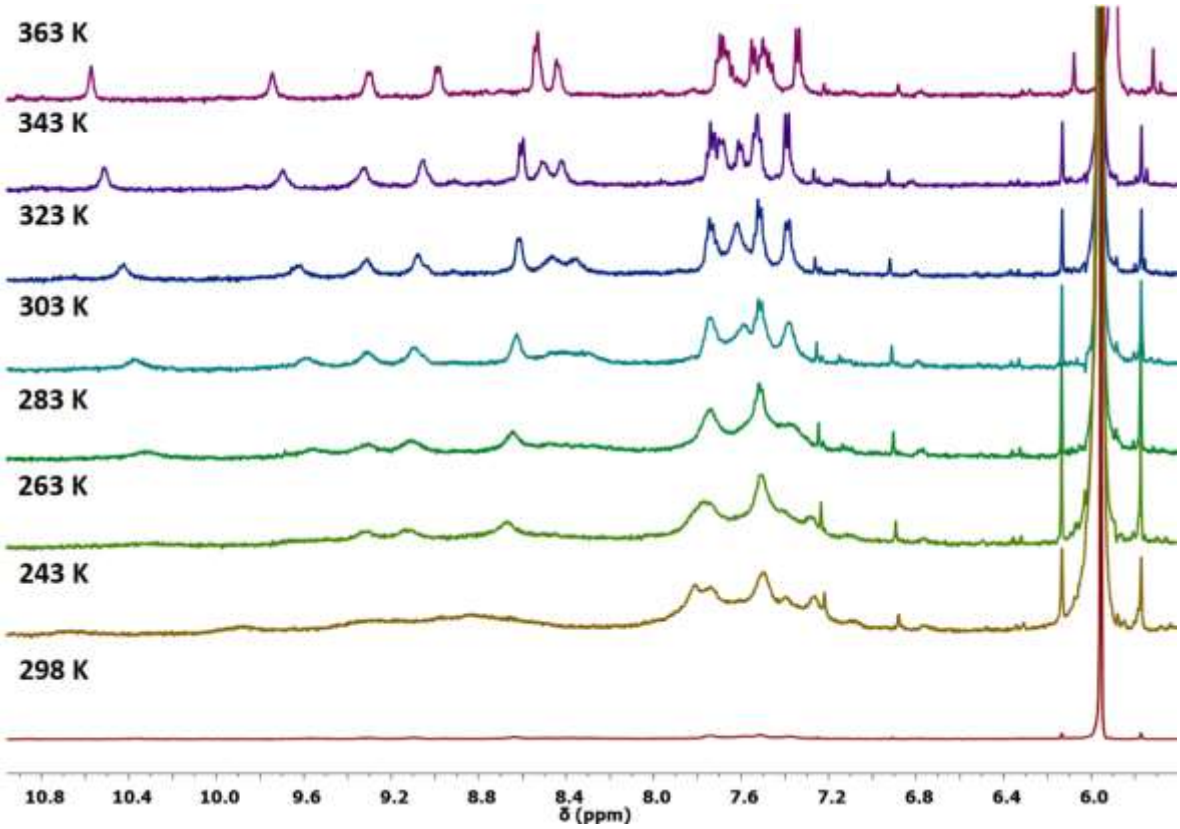

Figure S31. Variable temperature ^{1}H NMR spectra of **TDI-cDBT** (500 MHz, $C_2D_2Cl_4$).

VII. Mass Spectra

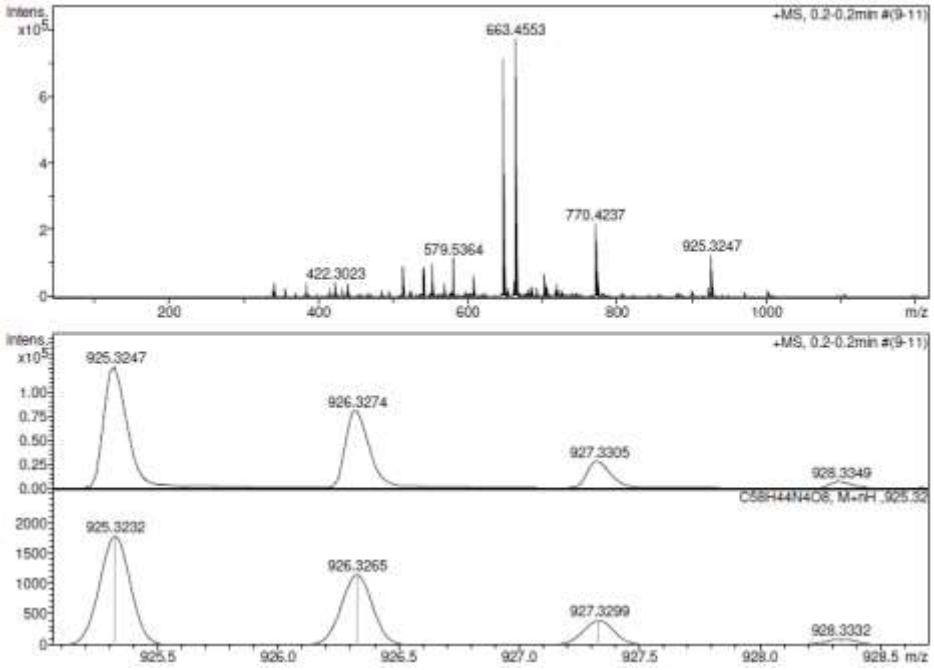

Figure S32. APCI-HRMS spectra of **1,6-TDI-(NO$_2$)$_2$**.

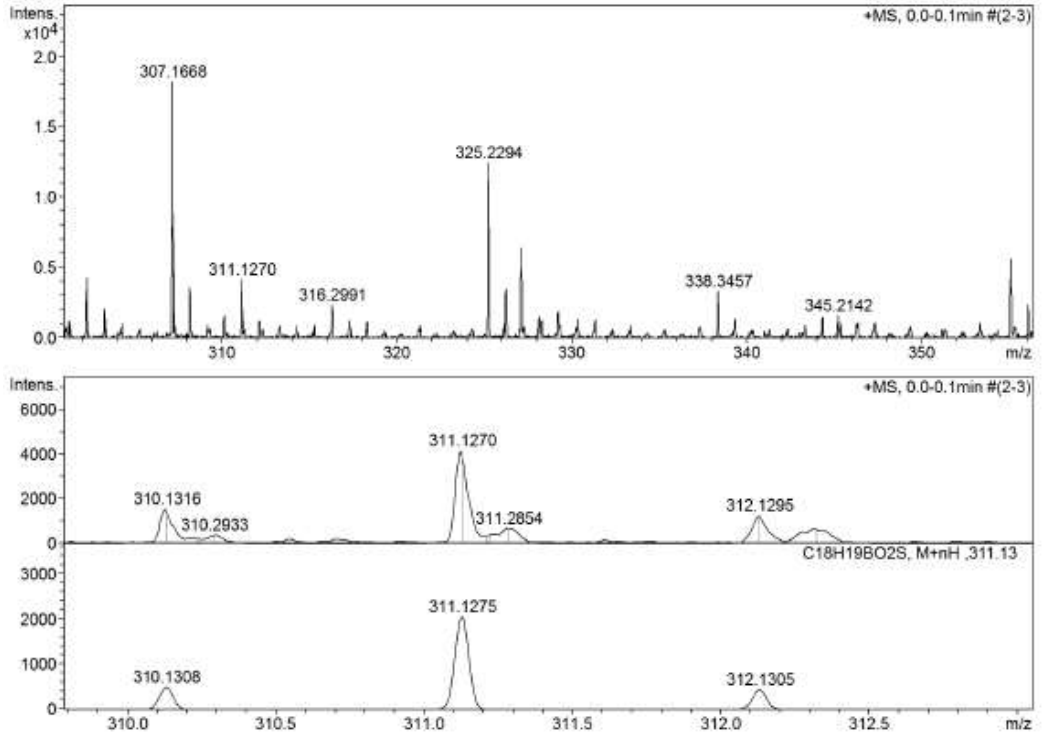

Figure S33 APCI-HRMS spectra of **DBT-B**.

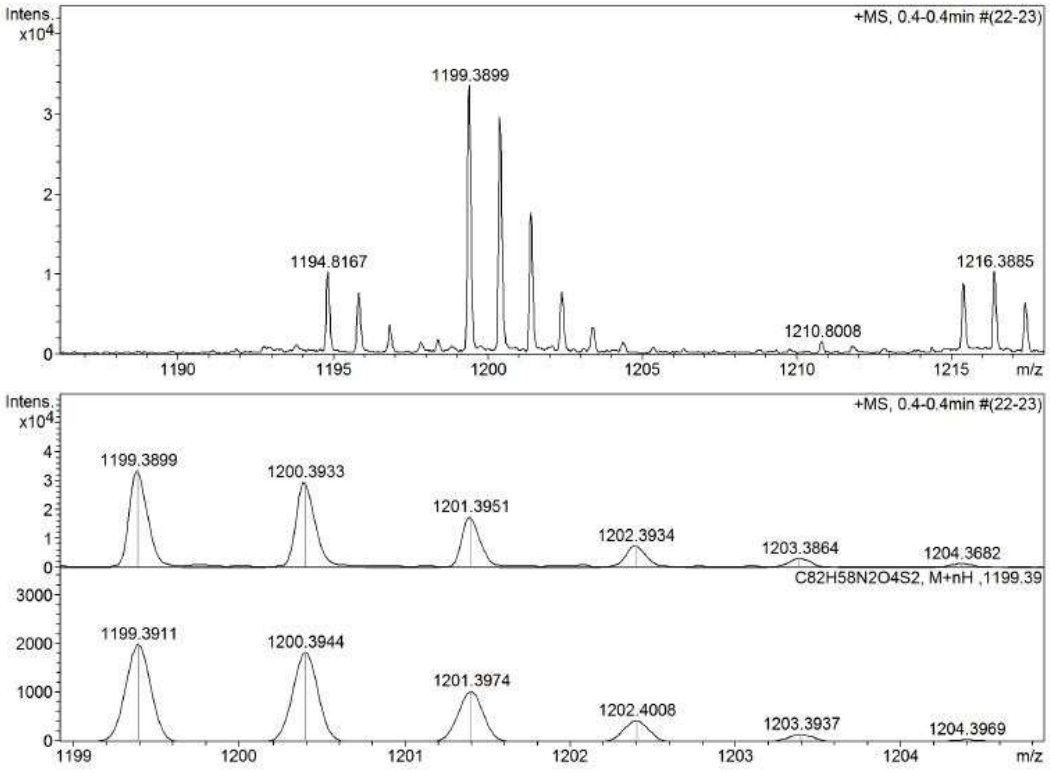

Figure S34. APCI-HRMS spectra of **TDI-sDBT**.

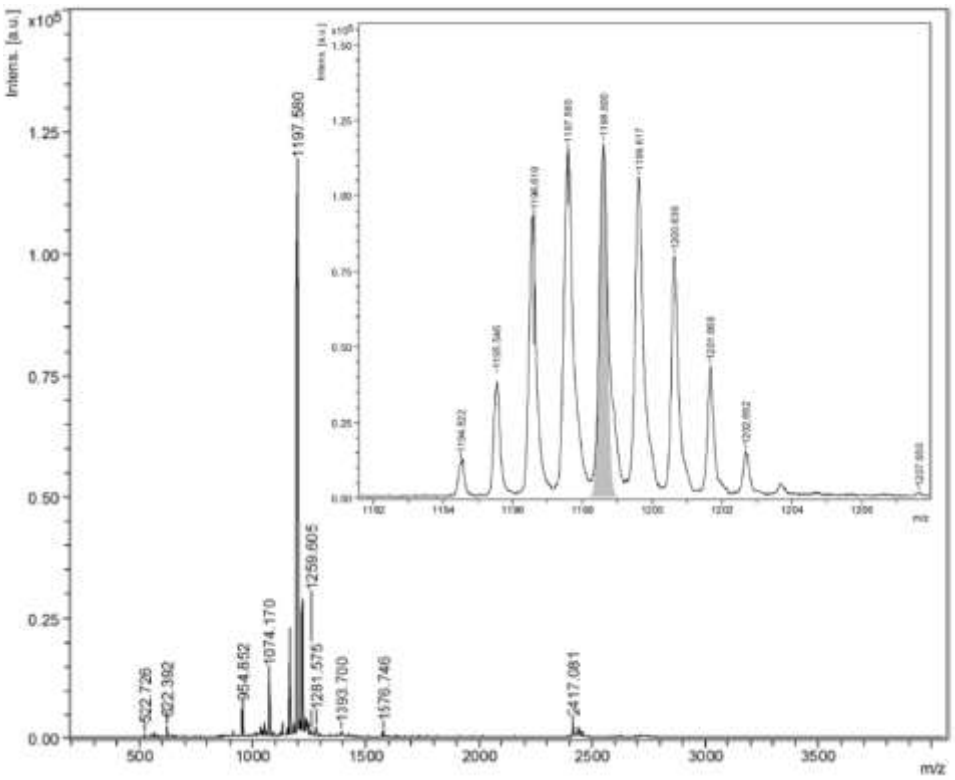

Figure S35. MALDI-TOF spectra of **TDI-scDBT**.

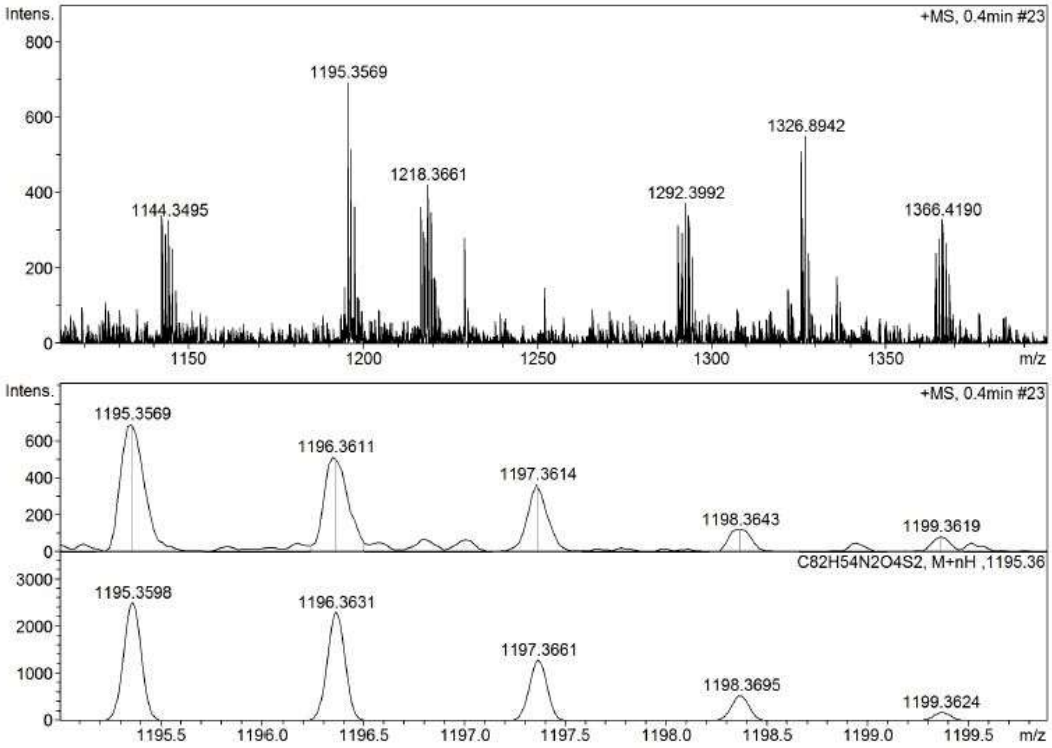

Figure S36. APCI-HRMS spectra of **TDI-cDBT**.

VIII. References:

(1) A. Lausi, M. Polentarutti, S. Onesti, J. R. Plaisier, E. Busetto, G. Bais, L. Barba, A. Cassetta, G. Campi, D. Lamba, A. Pifferi, S. C. Mande, D. D. Sarma, S. M. Sharma and G. Paolucci, *Eur. Phys. J. Plus,* 2015, **130**, 1-8.

(2) W. Kabsch XDS. *Acta Crystallogr. D,* 2010, **66**, 125-132.

(3) O. V. Dolomanov, L. J. Bourhis, R. J. Gildea, J. A. K. Howard and H. Puschmann, *J. Appl. Crystallogr.,* 2009, **42**, 339-341.

(4) G. M. Sheldrick, *Acta Crystallogr. Sect. A Found. Adv.,* 2015, **71**, 3-8.

(5) G. M. Sheldrick, *Acta Crystallogr. Sect. C Struct. Chem.,* 2015, **71**, 3-8.

(6) M. J. Frisch, G. W. Trucks, H. B. Schlegel, G. E. Scuseria, M. A. Robb, J. R. Cheeseman, G. Scalmani, V. Barone, B. Mennucci, G. A. Petersson, H. Nakatsuji, M. Caricato, X. Li, H. P. Hratchian, A. F. Izmaylov, J. Bloino, G. Zheng, J. L. Sonnenberg, M. Hada, M. Ehara, K. Toyota, R. Fukuda, J. Hasegawa, M. Ishida, T. Nakajima, Y. Honda, O. Kitao, H. Nakai, T. Vreven, J. A. Montgomery Jr., J. E. Peralta, F. Ogliaro, M. Bearpark, J. J. Heyd, E. Brothers, K. N. Kudin, V. N. Staroverov, R. Kobayashi, J. Normand, K. Raghavachari, A. Rendell, J. C. Burant, S. S. Iyengar, J. Tomasi, M. Cossi, N. Rega, J. M. Millam, M. Klene, J. E. Knox, J. B. Cross, V. Bakken, C. Adamo, J. Jaramillo, R. Gomperts, R. E. Stratmann, O. Yazyev, A. J. Austin, R. Cammi, C. Pomelli, J. W. Ochterski, R. L. Martin, K. Morokuma, V. G. Zakrzewski, G. A. Voth, P. Salvador, J. J. Dannenberg, S. Dapprich, A. D. Daniels, Ö. Farkas, J. B. Foresman, J. V. Ortiz, J. Cioslowski and D. J. Fox, Gaussian 09, Revision D.01, *Gaussian, Inc.* Wallingford CT, 2013.

(7) D. H. Oh, J. Park, H. Cho, G. Lee, D. Kim, J. Park, S. Lee and S. Hwang (DUK SAN NEOLUX CO., LTD.), US20210288262**,** 2021.

(8) K. S. Mehra, S. Jha, A. M. Menon, D. Chopra and J. Sankar, *Chem. Sci.,* 2023, **14***,* 3147-3153.

(9) M. Bendikov, H. M. Duong, K. Starkey, K. N. Houk, E. A. Carter and F. Wudl, *J. Am. Chem. Soc.,* 2004,**126**, 7416-7417.

(10) M. Adachi and Y. Nagao, *Chem. Mater*., 2001, **13**, 662-669.

(11) J. Hachmann, J. J. Dorando, M. Avilés and G. K.-L. Chan, *J. Chem. Phys.,* 2007, **127**, 134309.

(12) C. U. Ibeji and D. Ghosh, *Phys. Chem. Chem. Phys*., 2015, **17**, 9849-9856.

(13) M. Rano, S. K. Ghosh and D. Ghosh, *Chem. Sci.,* 2019, **10**, 9270-9276.

(14) M. Dey and D. Ghosh, *J. Phys. Chem. L,* 2022, **13**, 50, 11795-11800.